Cell Metabolism
Article

Neuronal ER Stress Impedes Myeloid-Cell-Induced Vascular Regeneration through IRE1α Degradation of Netrin-1

François Binet,[1] Gaëlle Mawambo,[2] Nicholas Sitaras,[1] Nicolas Tetreault,[4] Eric Lapalme,[1] Sandra Favret,[1] Agustin Cerani,[2] Dominique Leboeuf,[3] Sophie Tremblay,[1] Flavio Rezende,[1] Aimee M. Juan,[1] Andreas Stahl,[5] Jean-Sebastien Joyal,[1] Éric Milot,[2] Randal J. Kaufman,[6] Martin Guimond,[3] Timothy E. Kennedy,[4] and Przemyslaw Sapieha[1,2,4,*]
[1]Department of Ophthalmology
[2]Department of Biochemistry
[3]Department of Immunology
Maisonneuve-Rosemont Hospital Research Centre, University of Montreal, Montreal, QC H1T 2M4, Canada
[4]Department of Neurology and Neurosurgery, McGill University, Montreal, QC H3A 2B4, Canada
[5]University Eye Hospital Freiburg, Killianstrasse 5, 79106 Freiburg, Germany
[6]Sanford-Burnham Medical Research Institute, La Jolla, CA 92037, USA
*Correspondence: mike.sapieha@umontreal.ca
http://dx.doi.org/10.1016/j.cmet.2013.02.003

SUMMARY

In stroke and proliferative retinopathy, despite hypoxia driven angiogenesis, delayed revascularization of ischemic tissue aggravates the loss of neuronal function. What hinders vascular regrowth in the ischemic central nervous system remains largely unknown. Using the ischemic retina as a model of neurovascular interaction in the CNS, we provide evidence that the failure of reparative angiogenesis is temporally and spatially associated with endoplasmic reticulum (ER) stress. The canonical ER stress pathways of protein kinase RNA-like ER kinase (PERK) and inositol-requiring enzyme-1α (IRE1α) are activated within hypoxic/ischemic retinal ganglion neurons, initiating a cascade that results in angiostatic signals. Our findings demonstrate that the endoribonuclease IRE1α degrades the classical guidance cue netrin-1. This neuron-derived cue triggers a critical reparative-angiogenic switch in neural macrophage/microglial cells. Degradation of netrin-1, by persistent neuronal ER stress, thereby hinders vascular regeneration. These data identify a neuronal-immune mechanism that directly regulates reparative angiogenesis.

INTRODUCTION

Central neurons require a secure metabolic supply to ensure adequate function and transmission of sensory information. The breakdown of vascular beds in ischemic conditions such as stroke and proliferative retinopathies prevents nutrient and oxygen delivery and leads to hypoxic/ischemic events and a constellation of biochemical changes that compromises cellular function (Eichmann and Thomas, 2012; Lo, 2008; Moskowitz et al., 2010; Sapieha, 2012, Sapieha et al., 2010a). While the ensuing hypoxia is a potent stimulator of vascular growth itself (Lange et al., 2011; Ritter et al., 2006; Sapieha et al., 2010a, 2010b), initial attempts to revascularize the ischemic nervous tissue are typically inadequate (Fukushima et al., 2011; Joyal et al., 2011). Promoting faster revascularization is of great therapeutic interest, as this will decrease the damage secondary to ischemia and could prevent the destructive hypoxia-driven pathological neovascular phase associated with diseases such as diabetic retinopathy and retinopathy of prematurity (ROP).

In the central nervous system (CNS), one cellular manifestation of hypoxia/ischemia is endoplasmic reticulum (ER) stress (Chen et al., 2008; Hayashi et al., 2005; Paschen and Doutheil, 1999; Tajiri et al., 2004), which activates a collection of signaling pathways that initially promote cellular survival in a compromised metabolic situation. When ER homeostasis is perturbed, the unfolded protein response (UPR) is initiated and activates phosphorylation of protein kinase RNA-like ER kinase (PERK) and inositol-requiring enzyme-1α (IRE1α) (Bernales et al., 2006; Marciniak and Ron, 2006; Ron and Walter, 2007; Schröder and Kaufman, 2005). Together, these pathways signal to reduce the workload of folding machinery inside the ER (Figure 1A). ER stress is a short-term adaptive response, yet if it persists and is not resolved, it will contribute to tissue dysfunction (Tabas and Ron, 2011; Xu et al., 2005). To date, the physiological repercussions of ER stress have largely been investigated in the context of insulin resistance (Lee et al., 2011), atherosclerosis (Tabas, 2010), or liver disease (Malhi and Kaufman, 2011) while its influence in neurovascular homeostasis remains undefined.

The retina is a relevant model in which to study CNS neurovascular crosstalk due to its highly stereotyped apposition of central neurons, capillaries, venules, arteries, and veins (Dorrell and Friedlander, 2006; Joyal et al., 2011; Sapieha, 2012) (Figure S1A). Moreover, of immediate clinical relevance, compromised neurovascular networks result in proliferative retinopathies (PRs) such as diabetic retinopathy (Aiello, 2005) and retinopathy of prematurity (Sapieha et al., 2010b), which are the principal blinding diseases affecting pediatric and working-age populations in

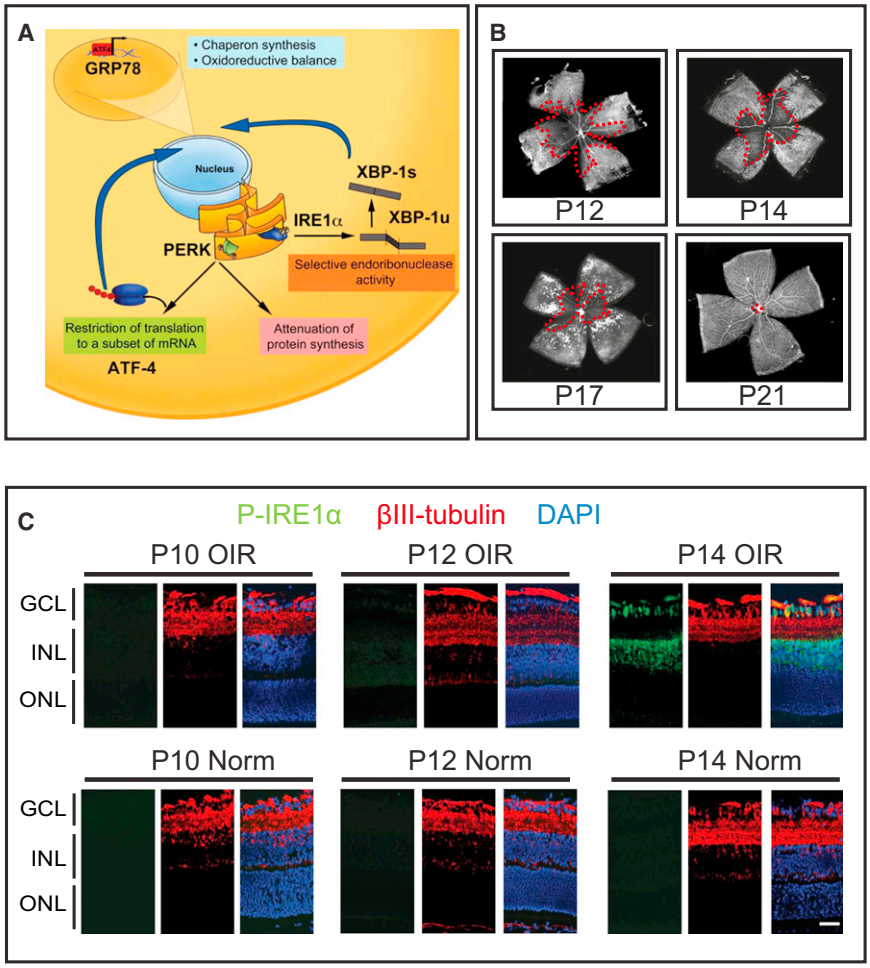

Figure 1. Neuronal ER Stress Is Induced in Hypoxic Retinas and Associated with Failure of Revascularization

(A) Graphic depiction of canonical ER stress pathways. The PERK arm controls ATF4 expression while IRE1α mediates XBP1 splicing. Both lead to GRP78 expression.

(B) Representative photomicrographs of isolectin B4-stained flatmount retinas from the OIR model illustrate the progression of vascular growth following initial vasoobliteration. Upon exit from O_2 at P12, the retina attempts to revascularize, yet there is an initial stall in regrowth followed by pathological preretinal neovascularization (white sprouts) that peaks at P17. Successively, vessels enter the avascular retina toward P19–P21, and the preretinal neovascularization regresses.

(C) Sagittal retinal sections show that phosphorylated IRE1α is robustly induced at P14 OIR and expressed in the retinal ganglion cell layer (GCL) as demonstrated by colocalization with βIII-tubulin-positive RGCs. P-IRE1α also stains cells of the inner nuclear layer (INL). Scale bar: 20 μm.

(D) Sagittal retinal sections show that phosphorylated PERK is induced at P14 OIR and expressed in the retinal GCL as demonstrated by colocalization with βIII-tubulin-positive RGCs.

(E) The expression of both markers is more robust in the avascular zones of the retina and does not colocalize with isolection B4 staining. ONL, outer nuclear layer; INL, inner nuclear layer; GCL, ganglion cell layer. Scale bar: 50 μm.

(F) Whole retinal cross-sections from P14 OIR confirm that p-IRE1α and p-PERK are expressed robustly in the central avascular area of the retina. Scale bar left panel: 20 μm, right panel: 500 μm. Images and analysis are representatives of three independent experiments.

(G) Sagittal sections of the retina showing the area harvested by LCM.

(H and I) ATF4 (H) and GRP78 (I) gene expressions are increased in OIR compared to normoxic littermates as determined by LCM of the ganglion cell layer of the retina.

(J) PERK and IRE1α are phosphorylated in response to hypoxia in cultured RGCs.

(K–M) ATF4 gene expression (K), XBP1 mRNA splicing (L), and GRP78 gene expression (M) are increased following prolonged hypoxic exposure (n = 4 independent experiments for each gene studied). $^{**}p < 0.01$ and $^{***}p < 0.001$. Values respresent a fold increase relative to time 0 hr ± SEM.

(N–P) During the phase of vascular dropout (P8), an injection of a lentivirus coding for an sh.IRE1α at P3 dramatically enhanced vascular regeneration (N) and decreased the preretinal neovascular area (O) in the regrowth phase of OIR at P17. Injection with a shPERK lentivirus did not result in any significant amelioration of vascular regeneration or reduction of preretinal neovascularization. Treatment with either sh.IRE1α or shPERK at P3 did not lead to noticeable variations in vasoobliteration (P). Representative images of retinas from each condition are presented. Scale bar: 1 mm. n = 8 animals/group; $^{*}p < 0.05$, $^{**}p < 0.01$, $^{***}p < 0.001$ relative to vehicle-treated retinas ± SEM.

industrialized countries (Gilbert et al., 1997; Kempen et al., 2004). PRs are generally characterized by initial microvascular degeneration followed by an excessive and pathological neovascularization provoked by the hypoxic retina attempting to reinstate oxygen and energy supply (Chen and Smith, 2007; Cheung and Wong, 2008; Smith, 2008). This attempted compensatory vascular regrowth is initially concentrated at the avascular border of the injured retina and hence fails to adequately perfuse the hypoxic tissue (Figure 1B). Instead, the new vessels are misdirected into the vitreous chamber, resulting in tangential sheering of the retina and consequent vision loss.

There has been a recent surge in our knowledge of the molecular mechanisms governing blood vessel growth (Carmeliet and Jain, 2011). During vascular development, several conserved regulatory cues are shared between neurons and vessels (Adams and Eichmann, 2010; Carmeliet and Tessier-Lavigne, 2005; Erskine et al., 2011; Larrivée et al., 2009; Miao et al., 1999; Soker et al., 1998). Vascular tip cells (Gerhardt et al., 2003) (analogous to axonal growth cones) probe and sense chemotropic attractant and repellent environmental cues and respond to the vascular endothelial growth factor (VEGF) by forming motile filopodia enriched in VEGFR2 and rich in guidance receptors for semaphorins (Neuropilins), netrins (UNC5B and DCC), ephrins (Ephs), and slits (roundabout) (Adams et al., 1999; Klagsbrun and Eichmann, 2005; Larrivée et al., 2009, 2007; Wilson et al., 2006). In addition, there is mounting evidence for the role of myeloid cells in vascular development (Stefater et al., 2011a, 2011b), repair (Checchin et al., 2006; Ritter et al.,

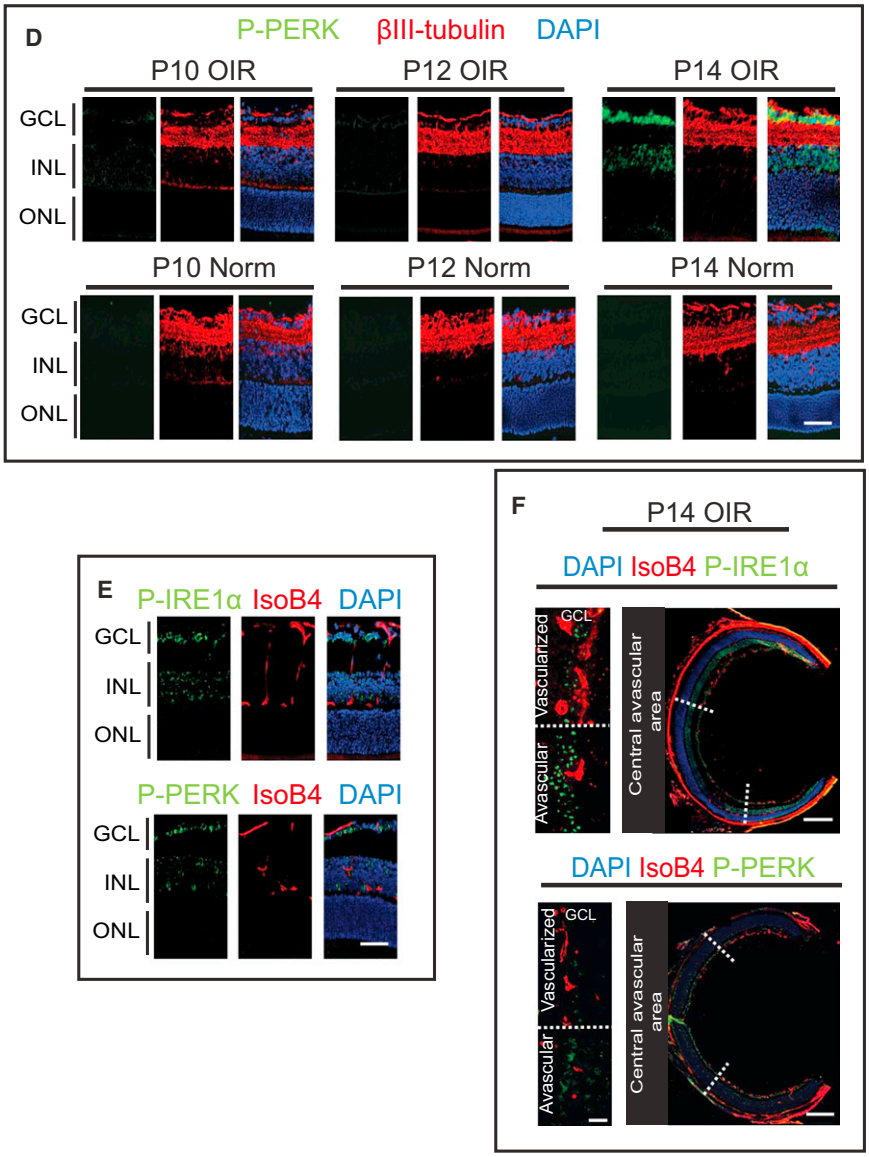

Figure 1. (*continued*).

dependent revascularization. Either inhibition of IRE1α or treatment with netrin-1 accelerates retinal vascular regeneration and consequently alleviates the hypoxic stimulus for destructive neovascularization. Our data reveal an inherent capacity of CNS neurons to repair neighboring tissue by summoning a reparative innate immune response and provide evidence for neuronal-immune communication in ischemic retinopathies. Approaches to foster revascularization may be desirable to counter ischemic stress in the CNS.

RESULTS

Neuronal ER stress Is Induced in Ischemic Conditions

The activation of canonical ER stress pathways is a conserved mechanism that enhances cellular survival under low metabolic conditions by reducing protein synthesis. This is achieved via phosphorylation of ER membrane-resident proteins such as PERK and IRE1α (Figure 1A). PERK restricts the translational machinery to a selected subset of messenger RNAs (mRNAs) such as ATF4, whereas phosphorylated, active IRE1α promotes splicing of XBP1 into an active transcription factor (XBP1s) that promotes expression of genes involved in UPR while the unspliced form (XBP1u) blocks transcription of genes involved in UPR. ATF4 and XBP1s induce transcription of specific homeostasis genes, such as the chaperone GRP78, to increase the protein-folding capacity of the ER (Figure 1A) (Ron and Walter, 2007). To determine if ischemia in central nervous tissue can provoke ER stress, we used the mouse model of OIR (75% oxygen from P7–P12 [postnatal day 7–12] and room air until P17), which yields a central avascular retina (Smith et al., 1994). This vascular degeneration is followed by a second phase of deregulated (albeit compensatory) vascular regeneration (Figure 1B). The secondary regrowth occurs upon return to room air (P12) for a period of approximately 7 days (Stahl et al., 2010).

We initially performed a time course for the expression of classical markers of ER stress throughout OIR. We focused on time points corresponding to the hyperoxic vasoobliterative phase (P10), upon return to normal air (P12), and in the initial phase of progressive vascular regrowth (P14). Phosphorylated PERK and IRE1α were found primarily in the ganglion cell layer (GCL) and colocalized with the RGC marker βIII-tubulin (Figures 1C and 1D). The phosphorylation was evident in P14 OIR retinas

2006), remodeling (Lang and Bishop, 1993), and anastomosis (Fantin et al., 2010) where these cells associate directly with vessels at the vascular front to exert their modulatory effects. To date, the influence of guidance cues on myeloid-induced vascular growth and remodeling has not been addressed.

Using the neural retina and its vascular system as a model of central neurovascular interaction, we set out to determine the outcome of hypoxia-induced neuronal ER stress on the vascular beds that perfuse this highly metabolic tissue. Employing the oxygen-induced retinopathy (OIR) model of vascular degeneration and regeneration (Smith et al., 1994), which serves as a proxy for human proliferative retinopathies such as diabetic retinopathy and retinopathy of prematurity, we uncovered a paradigm where ER stress in ischemic neurons provokes the suppression of vascular regeneration into hypoxic regions of CNS tissue. This results from an IRE1α-dependent downregulation of netrin-1, a protein we demonstrated to be required for myeloid-

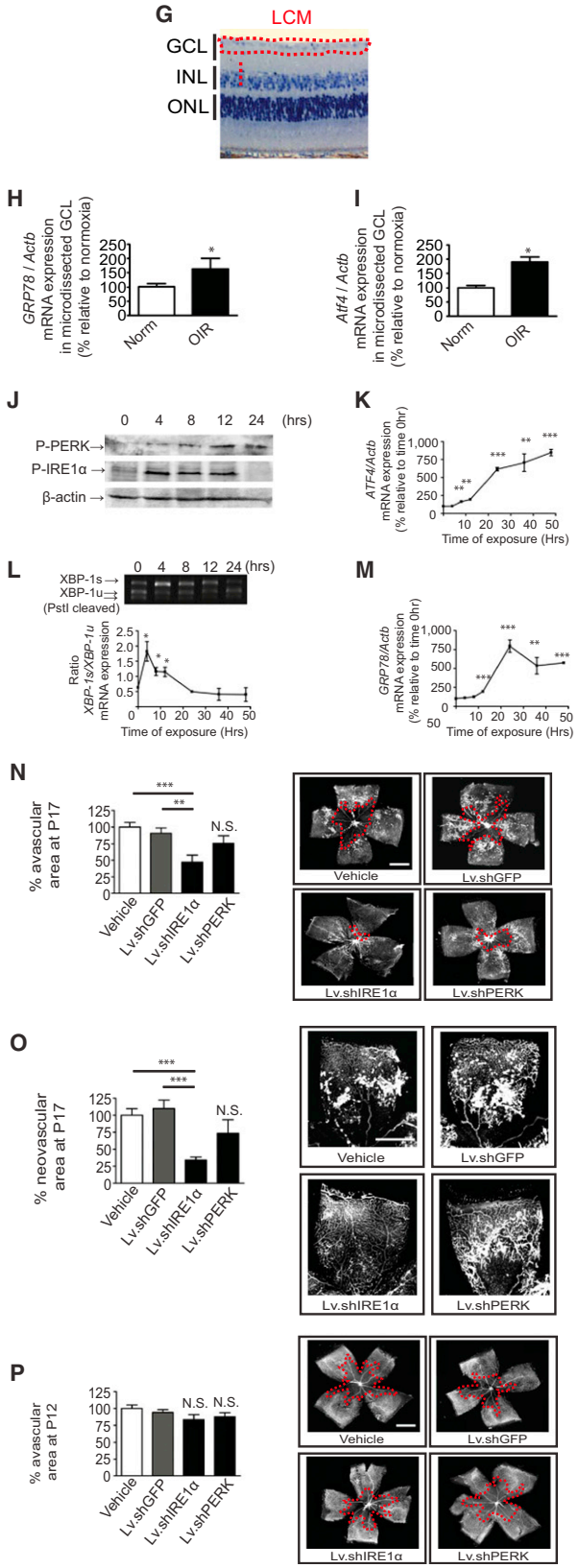

Figure 1. (*continued*).

during the early phase of vascular regeneration when reparative angiogenesis proceeds at a slow pace and the central retina remains hypoxic (Figures 1C and 1D). No phosphorylation of IRE1α and PERK was observed in the vascular layers (Figure 1E), highlighting the neuronal nature of the ER stress. This expression pattern was associated robustly with the central avascular area of the retina as confirmed with endothelial isolectin B4 staining (Figure 1F). Moreover, using laser capture microdissection (LCM), we specifically isolated the RGC layer from the retina (Figure 1G) and analyzed the expression of downstream effectors of ER stress pathways. Significantly enhanced expression of ATF4 and GRP78 transcripts was found in OIR mice compared to normoxic littermates at P14 (Figures 1H and 1I).

These findings were confirmed using an in vitro model of retinal neuron precursors cells (RGC-5) (Joyal et al., 2011; Sapieha et al., 2008) exposed to hypoxic conditions (1% O_2) in order to mimic the retinal ischemia present at P14 of OIR. First, we noted a pronounced phosphorylation of PERK and IRE1α (Figure 1J) representing the activation of ER stress pathways upon exposing RGC-5s to hypoxic conditions (starting at 4 hr). The activation of these pathways coincided with a marked upregulation of their effectors. ATF4 induction was detected at 8 hr and reached a greater than 8-fold increase in expression after 48 hr (Figure 1K). Concordantly, an increased splicing of XBP1 was observed, confirming the activation of IRE1α (ratio of 0.6327 at 0 hr and 1.826 at 4 hr of spliced versus unspliced XBP1 mRNAr) (Figure 1L). GRP78 expression was similarly elevated at 12 hr and increased by 8-fold at 24 hr (Figure 1M). The same pattern was noted for C/EBP homologous protein (CHOP), a transcription factor whose expression is controlled primarily by ATF4 and to a lesser extent by XBP1s (Oyadomari and Mori, 2004) (Figure S1B). Together, these findings indicate that the microvascular degeneration and ensuing ischemia characteristic of proliferative retinopathies triggers ER stress in retinal ganglion neurons.

Neuronal ER Stress Provokes Failure of Vascular Regeneration

Recent studies demonstrate that RGCs are important effector cells for retinal angiogenesis (Edwards et al., 2012; Fukushima et al., 2011; Joyal et al., 2011; Kim et al., 2011; Sapieha et al., 2008). We therefore sought to determine if ER stress in these neurons could influence retinal revascularization in OIR. To specifically hinder ER stress in RGCs in vivo, we generated lentiviral (Lv) vectors carrying small hairpin RNAs (shRNAs). These Lv vectors exhibit high tropism for RGCs when delivered intravitreally (Joyal et al., 2011; Sapieha et al., 2008) (Figure S2A). A single intravitreal injection of lentivirus shIRE1α (Lv.shIRE1α) or Lv.shPERK at P7 led to a significant reduction in IRE1α and PERK expression in whole retinas (Figures S2B and S2C, respectively). Lv.shIRE1α injections robustly enhanced retinal vascular regeneration by 3.7-fold compared to vehicle-treated controls (as determined by the extent of remaining avascular areas at P17; Figure 1N). Importantly, the enhanced rate of reparative angiogenesis profoundly reduced destructive preretinal neovascularization associated with ischemic retinopathies by over 65% (Figure 1O). This is likely attributed to the alleviation of hypoxic stress. Conversely, injections of Lv.shPERK did not result in any significant changes in retinal vascularization

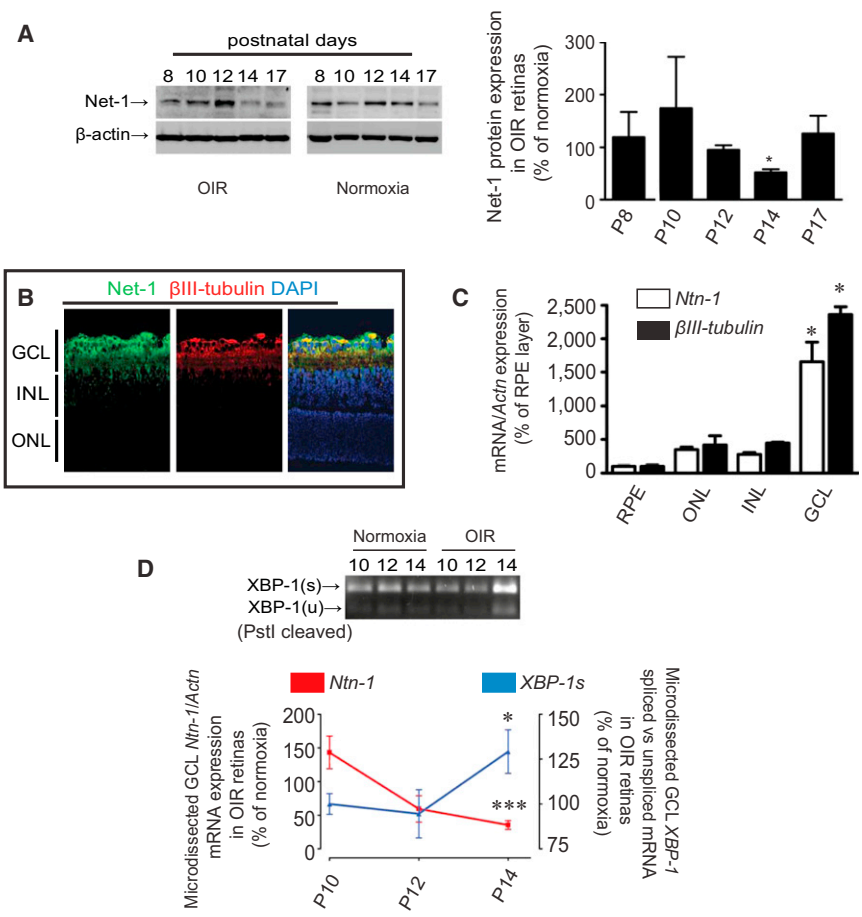

Figure 2. Netrin-1 Is Downregulated by Hypoxia-Triggered ER Stress

(A–C) Retinal Netrin-1 protein levels (western blot) drop during periods associated with elevated ER stress and vascular regeneration failure in OIR. n = 4 retinas/group, *p < 0.05 relative to normoxia. Netrin-1 is predominantly expressed in the retinal ganglion cell layer and colocalizes with βIII-positive RGCs, as assessed by IHC (B) and LCM (C). RPE = retinal pigment epithelium (representative of three independent experiments; P10 normoxic mouse eye). Scale bar, 50 μm; *p < 0.05.

(D) The drop in netrin-1 expression correlates with increased splicing of IRE1α in the ganglion cell layer isolated by LCM. *p < 0.05, ***p < 0.001 relative to normoxic controls and normalized to P10 ± SEM. n = 3 independent experiments.

(E and F) Netrin-1 gene expression is significantly reduced at P14 OIR (E) but preserved in Lv.sh.IRE1α-injected retinas (F). VEGF expression is not altered by Lv.shPERK and Lv.shIRE1α injections at P14 of OIR. n = 4 retinas. Injection of Lv.sh.PERK does not induce any significant change in netrin-1 gene expression. N.S., not significant; *p < 0.05, **p < 0.01 relative to normoxic vehicle or lv.shGFP-injected retinas ± SEM.

(G) Temporal gene expression of netrin-1 and VEGF in hypoxic cultured RGC-5 demonstrate the gradual increase of VEGF and the sharp drop in netrin-1. n = 4 independent experiments; *p < 0.05, ***p < 0.001 relative to time 0 hr ± SEM.

(H) Lv.shIRE1α preserves netrin-1 mRNA against hypoxic exposure. Graph depicts netrin-1 gene expression after 8 hr of hypoxia in cultured RGCs stably expressing shRNAs for either PERK, IRE1, PERK and IRE1α, or controls. n = 5 independent experiments; *p < 0.05 relative to shGFP-transfected cells ± SEM.

(Figure 1N) or neovascular tuft formation (Figure 1O), highlighting the central role of IRE1α in the control of reparative retinal angiogenesis. Importantly, we did not observe any differences in the extent of vasoobliteration at P12 upon treatment with either Lv.shIRE1α or Lv.shPERK (Figure 1P), thus confirming that the observed ER stress is primarily affecting the second phase regeneration and not the initial phase of vascular degeneration. These findings illustrate that ER stress (more specifically IRE1α activity) in hypoxic retinal ganglion neurons contributes to stalling vascular regrowth. Inhibiting this neuron-associated stress directly impacts reparative vascularization and thus highlights the importance of neurovascular crosstalk in this model of ischemic retinopathies.

Netrin-1 Is Degraded in Hypoxic Conditions by ER Stress

ER stress has been classically described as evoking a nonspecific response to restore cellular function. However, growing evidence points to a degree of selectivity with specific substrates being preferentially targeted by the effectors of the ER stress response. This is the case specifically with the endoribonuclease activity of IRE1α (Han et al., 2009; Hollien and Weissman, 2006). Given the elucidation of key roles for neuronal guidance cues in retinal vascularization (Eichmann and Thomas, 2012; Fukushima et al., 2011; Jones et al., 2008; Joyal et al., 2011; Kim et al., 2011; Larrivée et al., 2007), we turned our attention to these molecules.

Upon subjecting mice to the OIR model, we observed that the neuronal guidance protein netrin-1 (Kennedy et al., 1994) was profoundly downregulated at P14 (Figure 2A), a time that corresponds to elevated ER stress and initial attempts at vascular restoration (Figure 1B). In the retina, netrin-1 is mainly produced in the ganglion cell layer and colocalizes with the RGC marker βIII-tubulin (Figure 2B). In addition, cells of the inner nuclear layer showed a modest level of netrin-1 expression. This was confirmed by performing LCM on retinal layers where netrin-1 expression was 16-fold higher in the ganglion cell layer when compared to the RPE layer. Cells of the outer and inner nuclear layers showed only modest expression of netrin-1 (Figure 2C). We also confirmed that the expression of netrin-1 mRNA drops in the GCL layer as determined in LCM-isolated samples from P14 OIR and compared to normoxic littermates (Figure 2D). Interestingly, this drop in netrin-1 correlates with an increase in IRE1α-mediated XBP1 splicing activity at P14 OIR and thus temporally links IRE1α activity with a drop in netrin-1 mRNA (Figure 2D). Importantly, the decrease in netrin-1 mRNA seen at P14 (Figure 2E) is largely prevented by lentivirus small hairpin (Lv.sh)-mediated knockdown of IRE1α following intravitreal injection (Figure 2F), an effect not seen with Lv.shPERK. These data

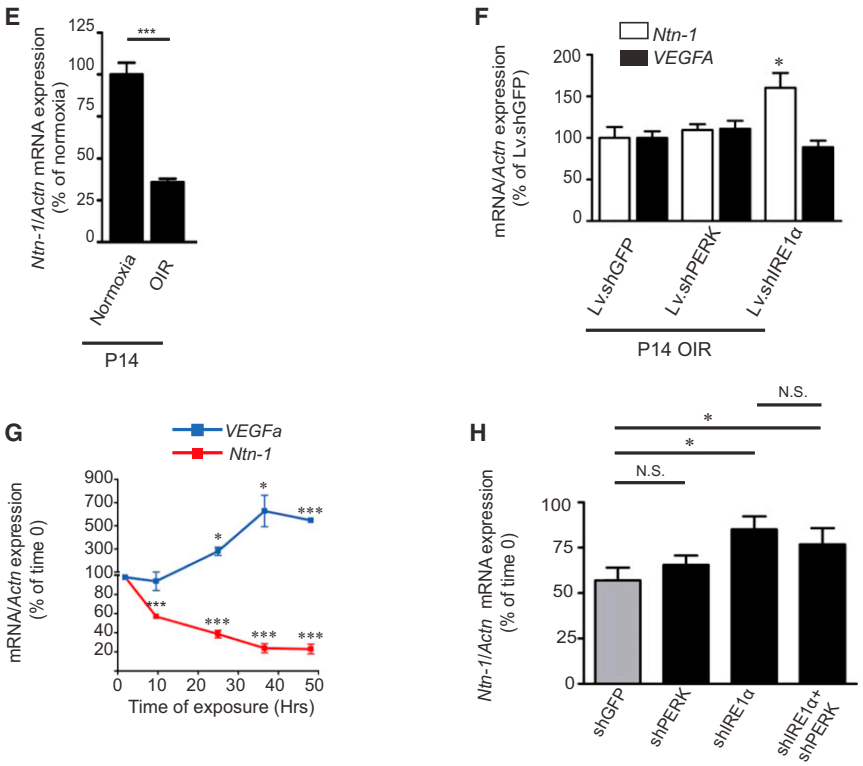

Figure 2. (*continued*).

identify a specific link between the IRE1α arm of the ER stress pathway and netrin-1. Moreover, as observed in whole retinal mRNA at P14 OIR, the degradation of netrin-1 by IRE1α is selective for netrin-1 since levels of VEGF are not affected by intravitreal administration of Lv.shPERK or Lv.shIRE1α (Figure 2F). While the levels of VEGF are not elevated in whole retinas, analysis at the microenvironmental level will be required to tease out the contribution of individual cell populations to VEGF production. Concordantly, netrin-1 decreases in cultured RGC-5s under hypoxic conditions (1% O_2) that mimic the ischemic phase of retinopathy while other transcripts such as VEGF increased as expected (Figure 2G). In this experimental paradigm, cultured RGC-5s were not serum starved in order to prevent premature induction of ER stress and UPR by amino acid deficiency.

To ascertain if ER stress pathways are responsible for the downregulation of netrin-1 in RGCs under hypoxic conditions, we generated PERK- and IRE1α-deficient RGCs by stable transfection with shRNA. Using these cell lines, we determined that IRE1α is the primary negative regulator of netrin-1 mRNA, as IRE1α-deficient cells showed significantly increased levels of netrin-1 under hypoxic conditions. Importantly, PERK-deficient cells or cells deficient for both PERK and IRE1α did not show any additional preservation of netrin-1 mRNA when compared to IRE1α alone, thus confirming the prominent role for IRE1α in the downregulation of netrin-1 (Figure 2H).

Netrin-1 Is Cleaved by the RNase Activity of IRE1α

Recent evidence suggests that the ribonuclease (RNase) activity of IRE1α, also termed IRE1-dependent decay (RIDD), specifically targets mRNAs encoding proteins that traverse the ER-Golgi secretory pathway (Hollien and Weissman, 2006). Therefore, to determine if netrin-1 could be a substrate for IRE1α, we cotransfected human embryonic kidney (HEK) cells that express endogenously low levels of netrin-1 (Shekarabi and Kennedy, 2002) with a plasmid encoding netrin-1 with or without an expression plasmid for IRE1α, a kinase-inactive/RNase-dead IREα (K599A), or an exclusively RNase-dead IRE1α (K907A) (Figure 3A) (Lipson et al., 2008). The overexpression of IRE1α drastically decreased the level of netrin-1 mRNA (Figure 3B), an effect also seen at the protein level (Figure 3C). In contrast, the degradation of netrin-1 was not observed with the kinase/endoribonuclease inactive dominant-negative mutant K599A (Lipson et al., 2008) or the endoribonuclease-dead mutant K907A (Figures 3B and 3C). In this experimental paradigm employing HEK cells, no effect was noted on the level of VEGF in the time frame (48 hr) investigated, demonstrating the selectivity of the reaction (Figures 3B and 3C). These results were confirmed by northern blot using a netrin-1-specific probe (Figure 3D).

IRE1α has been shown to target specific scission sites; these include 5′-CAGCAG-3′ in adjacent mRNA stem loops. This was demonstrated for the transcripts of mouse insulin II (Han et al., 2009) or makorin RING finger protein 2 (Oikawa et al., 2010). Using a bioinformatics approach, we generated the 2D structure of netrin-1 transcript (Figure 3E) and noted two putative cleavage sites for IRE1α in positions 1605–1610 and 1670–1675 located in stem loops (Figure 3E, red arrows). Exposure of cultured RGC-5s to hypoxia for 24 hr led to a substantial drop in netrin-1 mRNA as determined by semiquantitative PCR and was largely reversed when blocking IRE1α expression with shRNAs (Figure 3F). Netrin-1 fragments were very unstable using a cell transfection system, and no cleavage fragments were found by northern blot (Figure 3D), which could be due to the rapid activity of 5′-to-3′ and 3′-to-5′ exonucleases. We therefore employed a cell-free system to analyze the presence of these fragments using recombinant GST-fused IRE1α. We designed distinct sets of primers spanning the predicted sequences of IRE1α cleavage sites in netrin-1 mRNA. Loss of netrin-1 transcript was only observed when amplifying across the prospective IRE1α scission sites (959–1683 but not 511–891) (Figure 3G), thus confirming that IRE1α targets netrin-1. Together these data demonstrate that netrin-1 mRNA is a substrate for IRE1α.

Restoring Netrin-1 Accelerates Revascularization of the Ischemic Retina

Given the pronounced reduction of netrin-1 (noted above; Figure 2) during a period in which retinal revascularization is compromised (Joyal et al., 2011; Stahl et al., 2010), we sought

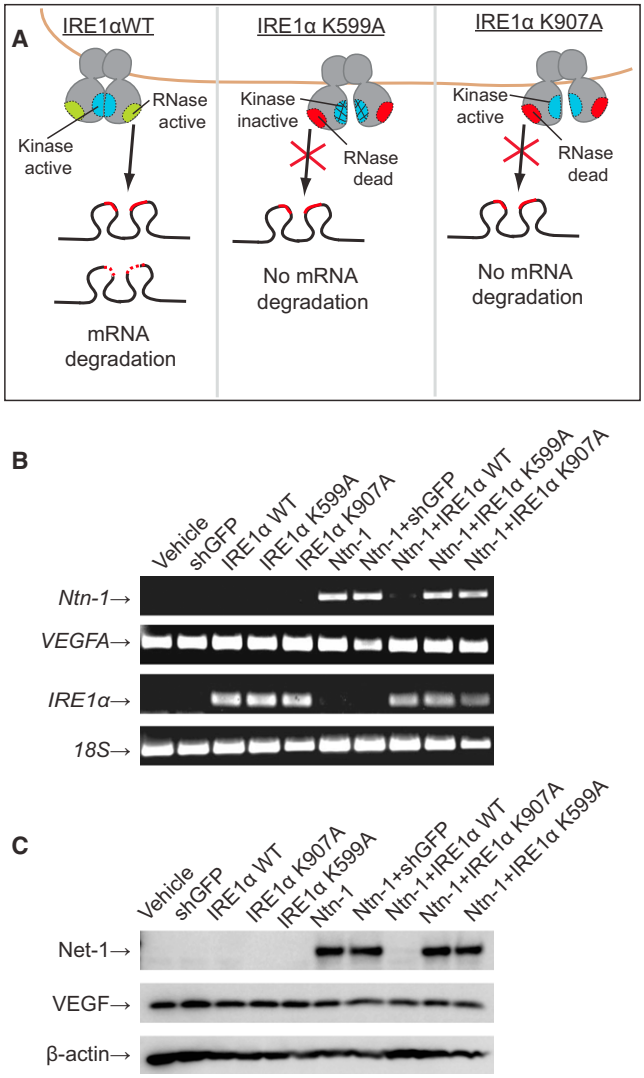

Figure 3. Netrin-1 Is Cleaved by the RNase Activity of IRE1α

(A) Schematic representation of IRE1α RNase activity following kinase activation, which can be abolished using a K599A or K907A mutant.

(B and C) Netrin-1 and IRE1α WT expression plasmid cotransfection results in the degradation of netrin-1 mRNA (B) and protein (C). Cotransfection with an IRE1α endoribonuclease/kinase-dead mutant (K599A), an endoribonuclease-inactivated mutant (K907A), or an irrelevant expression plasmid (shGFP) does not induce degradation of netrin-1 mRNA (B) or protein (C). VEGF mRNA (B) and protein (C) are not degraded by IRE1α activity. IRE1α is highly expressed following transfection with IRE1α WT, K599A, or K907A plasmids (third panel) (B).

(D) Northern blot showing degradation of the netrin-1 mRNA using the same conditions as in (B) and (C).

(E) 2D reconstitution of secondary structure of netrin-1 murine mRNA (position 1191–1960). Red arrows depict putative 5′-CAGCAG-3′ recognition sites for IRE1α RNase activity in stem loops (position 1605–1610 and 1670–1675). Each predicted base pair is colored with the heat color gradation from blue to red, indicating the base-pairing probability from 0 to 1.

(F) Netrin-1 mRNA degradation in hypoxic RGCs (1% O_2) can be reversed with an shRNA directed against IRE1α.

(G) Amplification products with primers spanning the putative cleavage sites (959–1683) show degradation of netrin-1 mRNA with recombinant IREα, an effect not seen with primers outside the cleavage sites (511–891). Panels (B), (C), (D), (F), and (G) are representative of at least three separate experiments.

to determine if restoring netrin-1 levels by ectopic intravitreal administration would enhance reparative angiogenesis following OIR. A single intravitreal injection of netrin-1 at P14 accelerated vascular regeneration and consequently decreased the avascular area of retina in a dose-dependent manner: 25% reduction with 50 ng/mL, 57% with 100 ng/mL, and 67% reduction with 200 ng/mL (Figure 4A). This rapid restoration of retinal vascularization lead to reduced pathological preretinal neovascularization with the 100 ng/ml dose abrogating close to 70% of this destructive angiogenesis (Figure 4B). To ascertain whether the regenerated vessels were healthy, we determined their barrier function by angiography with fluorescein isothiocyanate (FITC)-dextran. Regenerated vessels in netrin-1-injected retinas assumed a healthy disposition and did not present any signs of vascular leakage in contrast to vehicle-injected controls, which showed blebbing and poor retention of FITC-dextran (Figure 4C). These data attest to the stability of the neovessels in netrin-1-treated retinas.

To further confirm the role of netrin in retinal angiogenesis, we designed a lentiviral vector carrying an shRNA targeting netrin-1 and administered it to the developing retina. Intravitreal injection of Lv.shNtn1 at P2 significantly reduced the expression of netrin-1 at P7 (Figure S3A) and resulted in an abnormal vascular front with several retracted tip cells (Figure S3B, solid white arrows). Isolectin-B4-positive microglial cells were found in the general vicinity of the growing vascular front, yet were less in direct contact with vascular tip cells in Lv.shNtn-1-treated retinas (Figure S3B, gray dotted arrows). Taken with the previous, these data demonstrate that a specific substrate of neuronal ER stress, namely netrin-1, has potent vasoregenerative properties.

Netrin-1 Modulates the Expression of VEGF in Macrophage/Microglial Cells

To gain insight into the mechanisms by which netrin-1 accelerates retinal revascularization, we explored its influence on the prominent retinal proangiogenic factor VEGF (Pierce et al., 1995; Pierce et al., 1996). The same intravitreal injection of netrin-1 that significantly enhanced revascularization (Figure 4) induced a significant yet very modest increase in gene expression of VEGF in the total retina 24 hr postinjection (Figure 5A). Elevated panretinal levels of VEGF are associated with pathological ocular neovascularization (Aiello et al., 1995). However, we observed only a modest rise in retinal VEGF in our experimental paradigm. Yet this increase in VEGF precipitated reparative angiogenesis. We therefore sought to explore the source of the VEGF production at a microenvironmental level and elucidate which cell population was responsible for this netrin-1-induced production of VEGF.

Following administration of Myc-tagged recombinant netrin-1 protein to the vitreous as described above (Figure 4), we detected Myc-netrin-1 specifically localized to lectin and Iba1-positive microglia/macrophages at the vascular front (Figure 5B) in close proximity with tip cells (Figure 5B, white arrows). Confocal images were taken 3 hr postinjection. A 3D reconstruction shows the binding of exogenously applied netrin-1 to the cell surface of microglia/macrophages (Movie S1).

To determine whether netrin-1 can have biological effects on these cells, we evaluated the expression of netrin-1 receptors in a murine macrophage cell line (J774) (Figure 5C) and in primary

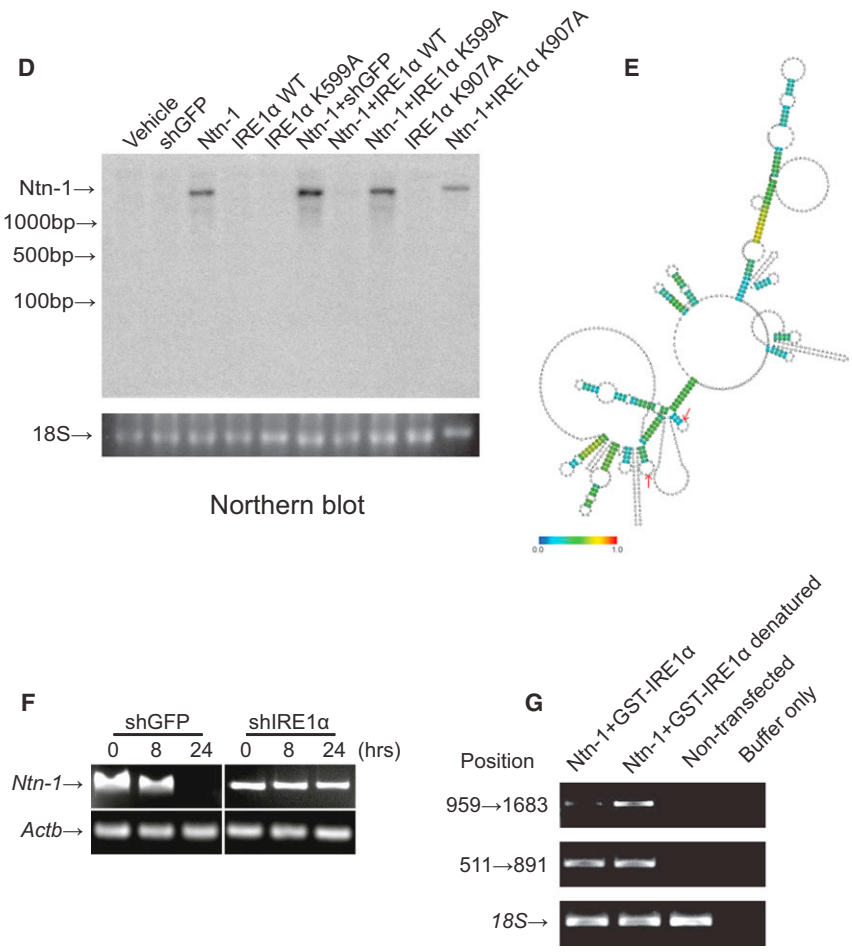

Figure 3. (*continued*).

microglia (Figure S4A). Our results demonstrate that UNC5B, neogenin, and the putative receptor for netrin, adenosine A2B receptor (AA2BR), are expressed in macrophages (Figure 5C), with a similar pattern in primary microglial cells (Figure S4A). Conversely, UNC5A and DCC are undetectable or negligibly expressed in macrophages or microglia. Macrophages may thus be required for netrin-1 to exert proangiogenic effects, as netrin-1 alone has been elegantly shown to inhibit sprouting angiogenesis (Larrivée et al., 2007).

We next analyzed the ability of netrin-1 to induce expression of VEGF and angiopoietins directly in macrophages. Netrin-1 (100 or 200 ng/ml) induced a 3-fold increase of VEGF expression in macrophages (Figure 5D). Moreover, a significant increase in other proangiogenic factors such as Angiopoietin 2 was noted while the vasostabilizing Angiopoietin 1 was affected minimally, suggesting a general proangiogenic modulation by Netrin-1 (Figure S4B). Increased expression of VEGF was induced similarly in primary microglia by application of netrin-1 (Figure S4C). Given that Angiopoietin 2 requires VEGF to induce angiogenic growth, we focused our study on VEGF. We therefore analyzed the expression of VEGF in the presence of various blockers of netrin-1 receptors. In this context, only the AA2BR antagonist PSB1115 or an AA2BR siRNA were able to decrease the induction of VEGF while neutralizing antibodies or siRNAs against UNC5B (Ly et al., 2005; Tadagavadi et al., 2010), and Neogenin (Lejmi et al., 2008) did not prevent this induction (Figure 5D). We verified that these siRNAs were transfected effectively in macrophages using siGLO and fluorescence-activated cell sorting (FACS) analysis (Figure 5D, inset) and certified their specificity and potency (Figure S4D).

To confirm that netrin-1 can exert a biological effect on macrophages, we analyzed the activation of the mitogen activated protein kinase (MAPK) ERK1/ERK2 as a generic readout of intracellular activity. Relevantly, ERK1 and ERK2 are known to be activated by the AA2BR (Yang et al., 2011) and stimulated following netrin-1 exposure to epithelial cells (Wang et al., 2009). Treatment of macrophages with a 100 ng/mL dose of netrin-1 induced a rapid increase of ERK1/ERK2 phosphorylation starting at 5 min and peaking at 30 min (Figure 5E). Preincubation with PSB1115 reversed ERK1/ERK2 phosphorylation (Figure 5F), confirming the involvement of this receptor in netrin-1-mediated signaling in macrophages. These data reveal that netrin-1 can prompt myeloid cell production of proangiogenic factors such as VEGF. This provides a paradigm in which netrin-1 induces an angiogenic switch in microglial cells and drives reparative angiogenesis at a microenvironmental level, thus promoting localized vascular regeneration without increasing overall pathological angiogenesis.

The Proangiogenic Properties of Netrin-1 Are Driven by Macrophages

To investigate the contribution of macrophages to the proangiogenic effects of netrin-1, we conducted a series of ex vivo and in vitro angiogenesis assays. Cultured macrophages were exposed to 100 ng/mL netrin-1 for a period of 24 hr and used to condition fresh culture media (Figure 6A). The conditioned media (CM) containing factors secreted by macrophages secondary to netrin-1 stimulation was collected, filtered, and used to culture human retinal microvascular endothelial cells (HRMECs). Using a CyQUANT Cell Proliferation Assay, we found that supernatants from netrin-1-stimulated macrophages induced a robust 30-fold induction in HRMEC proliferation compared to nonstimulated controls (Figure 6B). In line with the results above, the AA2BR inhibitor, PSB1115, abolished the proliferative effects of netrin-1 (Figure 6B). Direct addition of netrin-1 lead to less pronounced endothelial proliferation, suggesting that the proangiogenic effects of CM are mediated by factors produced by netrin-1-stimulated macrophages and not by exogenously added netrin-1. In order to confirm the

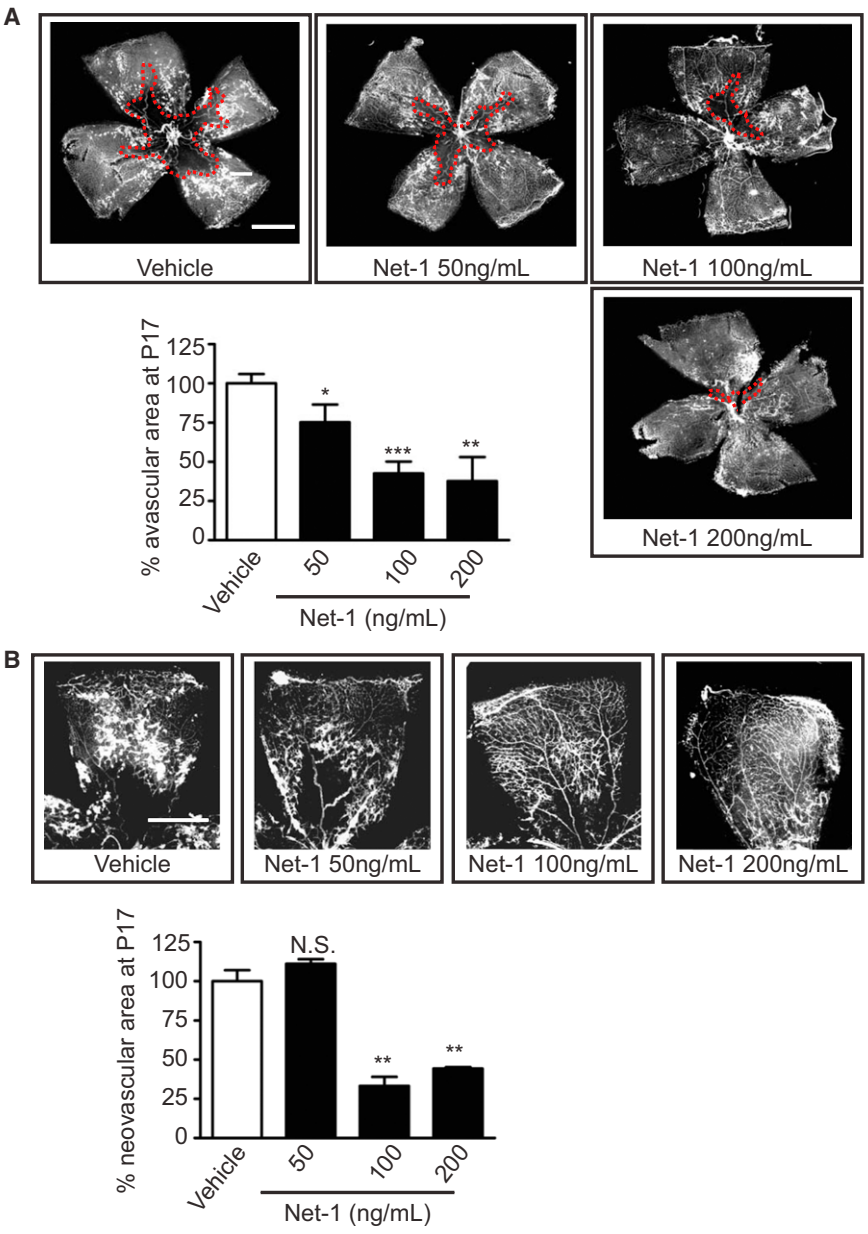

Figure 4. Administration of Netrin-1 to Ischemic Retinas Enhances Vascular Regeneration and Suppresses Pathologic Neovascularization

(A and B) Isolectin B4 stained retinas from P17 mice injected intravitreally at P14 with 50, 100, or 200 ng/mL of recombinant netrin-1 or vehicle (PBS). Netrin-1 effectively enhanced reparative angiogenesis (A) and diminished neovascular areas (B) as determined at P17. Representative images of retinas for each condition are presented. n = 10–13 animals/group for each calculation; *p < 0.05, **p < 0.01,***p < 0.001 relative to vehicle-injected retinas ± SEM. Scale bar: 1 mm. (C) Neovessels induced by netrin-1 treatment do not show any signs of leakage of FITC-dextran, as opposed to vehicle-injected retinas. Representative images of three independent experiments. Scale bar: 100 μm.

angiogenic potential of netrin-1-stimulated macrophages in vivo, we used a Matrigel plug assay in which CM was solubilized with Matrigel and injected subcutaneously in mice. Ten days following introduction of plugs, mice were perfused with FITC-dextran, and the extent of invading vascularization was quantified by spectrofluorometry. Netrin-1 CM induced a 4-fold increase in plug angiogenesis (Figure 6C), an effect visualized by fluorescent microscopy (Figure 6C). Consistent with the data above, inhibition of AA2BR efficiently abolished the capacity of netrin-1 to induce macrophage-dependent vascularization, as revealed by a decrease in vascular networks observed in PSB1115-CM-treated Matrigel plugs (Figure 6C).

Next, we verified if netrin-1 CM from macrophages could induce sprouting angiogenesis in aortic explants. The results presented in Figure 6D demonstrate that CM from macrophages incubated with netrin-1 significantly increased aortic ring sprouting area compared to controls. As above, the CM harvested from macrophages pretreated with PSB1115 provoked considerably less vascular growth, thus confirming the role of this receptor in netrin-1-induced angiogenesis (Figure 6D).

Importantly, consistent with previous studies (Larrivée et al., 2007), direct incubation of aortic explants with netrin-1 alone lead to a dose-dependent reduction in vascular sprouting (Figure S5). These results underscore the importance of macrophages in mediating the proangiogenic effects of netrin-1. Given the central role of VEGF in angiogenesis, including as a positive modulator of the effects of angiopoietins, we sought to determine if neutralization of VEGF would abrogate the proangiogenic effects of the CM from netrin-1-treated macrophages. Indeed, our data confirm that VEGF was the major proangiogenic effector in the CM, given that addition of a VEGF-neutralizing antibody reversed the observed sprouting angiogenesis (Figure 6E), an effect not seen with addition of a control goat immunoglobulin G (IgG) antibody. Combined, the findings presented in Figure 6 provide evidence that the direct effect of netrin-1 on proliferation and migration of endothelial cells was either not significant or negligible compared to the pronounced effect of netrin-1 CM that was obtained from macrophages. Moreover, we showed that VEGF is a central proangiogenic effector secreted by netrin-1-stimulated macrophages.

Neurovascular Regeneration by Netrin-1 In Vivo Is Macrophage/Microglial Cell Dependent

Retinal myeloid cells (macrophages/microglia) participate in vascularization both during development (Stefater et al., 2011a,

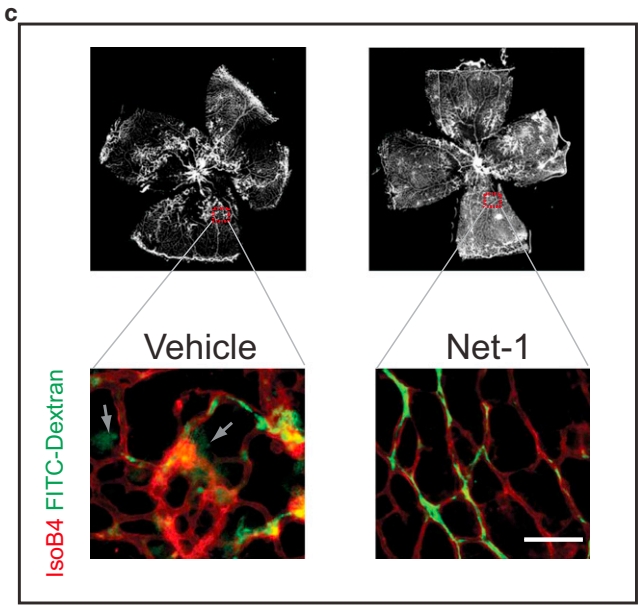

Figure 4. (*continued*).

2011b) and in pathological neovascularization (Stahl et al., 2010). To confirm that retinal macrophages/microglia mediate the observed netrin-1-induced vascular regeneration of the ischemic retina (Figure 4) and to further rule out a direct effect of netrin-1 on endothelium, we proceeded to deplete the retina of myeloid cells by intravitreal injection of clodronate liposomes prior to treatment with netrin-1. Clodronate liposomes have been used successfully to remove macrophages from distal organs (van Rooijen and van Kesteren-Hendrikx, 2002) as well as the retina (Ishida et al., 2003; Ritter et al., 2006). We first confirmed the ability of our clodronate liposome preparation to induce apoptosis of macrophages in vitro (Figure S6).

We next verified the efficacy with which clodronate liposomes deplete retinal macrophages/microglia by FACS analysis. Treatment with clodronate liposomes lead to a significant 2-fold reduction in retinal macrophages/microglia compared to control empty liposomes as confirmed by 7-AAD negative-F4-80/CD11b positive cells (~4,500 microglia for empty liposomes and ~2,300 microglia for clodronate liposomes/retina). 7-AAD negative cells are viable (Figure 7A).

As expected, intravitreal injection of netrin-1 enhanced vascular regeneration by ~50% as observed at P17 in empty-liposome-injected animals. Conversely, delivery of netrin-1 to macrophage/microglia-depleted retinas did not induce any significant difference in vascular regeneration, thus underscoring the importance of these immune cells in netrin-1-induced angiogenesis (Figure 7B). We next verified the contribution of the macrophage/macroglial-derived VEGF produced in response to netrin-1 (described in Figures 5 and 6). To this end, we simultaneously injected netrin-1 and anti-VEGF neutralizing antibodies and analyzed the outcome on vascular regeneration at P17. Blocking antibodies for VEGF effectively abolished the proregenerative effect of netrin-1, confirming the key role of this factor in the regeneration of the vasculature observed in our paradigm (Figure 7C). Our data indicate that netrin-1 activates an angiogenic switch in macrophages/microglia, and thus drives microenvironmental revascularization, but does not contribute to pathological preretinal neovascularization. Taken together, we demonstrate that sustained ER stress specifically targets netrin-1, which we identify as a potent retinal revascularization factor that mediates its effects through retinal myeloid cells.

DISCUSSION

The neurovascular unit has been increasingly investigated in health and disease over the course of the last decade. In this study, we put forward two concepts pertaining to the role of ER stress in hindering reparative angiogenesis within the CNS. First, we demonstrate that sustained neuronal ER stress, through the endoribonuclease IRE1α, provokes the degradation of netrin-1 and results in revascularization failure of the ischemic retina. Second, we present neuronal-derived netrin-1 as a potent mediator of myeloid-cell-induced CNS vascular regeneration (Figure 7C). Although mechanisms governing vascular degeneration and the ensuing preretinal neovascularization in proliferative retinopathies have been extensively studied (Ashton et al., 1954; Campbell, 1951; D'Amore and Sweet, 1987; Lundbaek et al., 1970; Michaelson, 1948; Simons and Flynn, 1999; Smith, 2004; Smith et al., 1994; Tesfamariam, 1994), there are no strategies to date to accelerate revascularization of the vaso-obliterated retina and consequently alleviate the ischemic stress that is central to disease progression. Gaining insight into why vascular regeneration stalls or proceeds at compromised rates will be key to understanding the pathomechanisms of ischemic neuropathies.

Hypoxia is an activator of the unfolded protein response in conditions such as ischemic heart disease or cerebral ischemia (Tajiri et al., 2004). We demonstrate that both arms of the ER stress response, IRE1α (cleavage of XBP1) and PERK (induction of ATF4), are profoundly induced in response to neuronal hypoxia. Although it is well established that mild hypoxia (via hypoxia-inducible factor [HIF]) drives a cluster of over 70 genes that encode proteins that promote the adjustment to an oxygen deficient state (Bruick, 2003; Lange and Bainbridge, 2012; Paul et al., 2004), it is conceivable that when the ischemic shock persists, the nervous tissue segregates irreversibly damaged regions in an attempt to deviate metabolic stores to less-affected and more-salvageable areas (Joyal et al., 2011). Globally, this concept may in part explain the production of vasorepulsive guidance cues in ischemic cores secondary to severe vascular injury in stroke (Fujita et al., 2001) or in vasodeficient areas of the retina in retinopathy (Fukushima et al., 2011; Joyal et al., 2011). The sustained activation of ER stress pathways, and specifically IRE1α, may provide the neuron with the appropriate enzymatic machinery to shift from a prosurvival program to one that repels vessels and thus redistributes oxygen and nutrients to sectors of tissue that would preferentially benefit. In agreement, degradation of netrin-1 transcripts by IRE1α during a state of sustained hypoxia perturbs revascularization and thus permits vasorepellant factors such as semaphorins 3A and 3E to deviate nascent angiogenic sprouts from severely ischemic areas of nervous tissue (Fukushima et al., 2011; Joyal et al., 2011).

The paradigm we present suggests that the cellular consequences of ER stress are finely tuned and selective. In an attempt

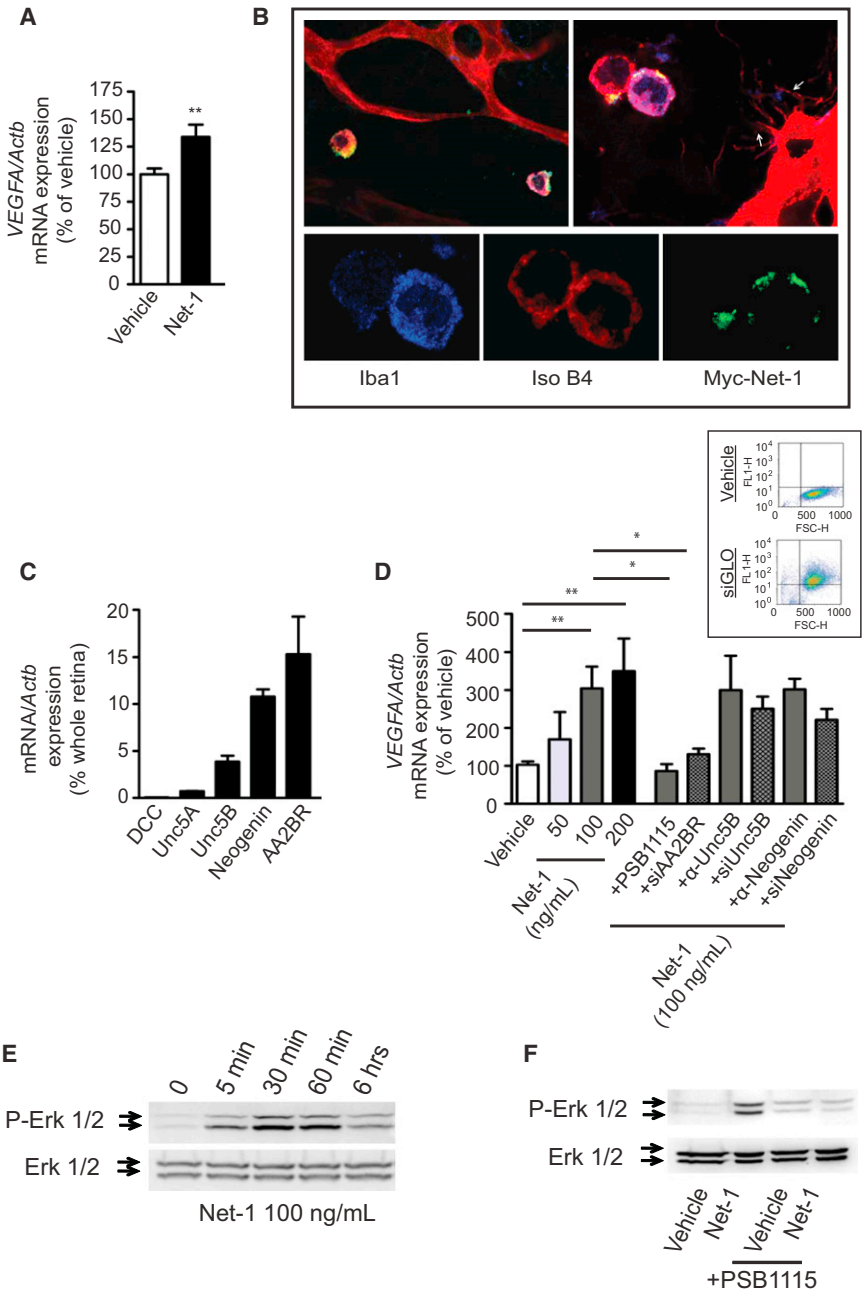

Figure 5. Netrin-1 Activates AA2BR on Macrophages and Provokes the Release of VEGF in an ERK1/ERK2-Dependent Manner

(A) Intravitreal injection of netrin-1 (100 ng/mL at P14) induces retinal VEGF gene expression at P15 OIR. n = 6 animals/group; **p < 0.01 relative to vehicle injected retinas ± SEM.

(B) Confocal images of c-Myc-tagged netrin-1 reveals binding to Iba1-positive macrophages/microglia 3 hr postinjection (P14 OIR). Representative images of three independent experiments.

(C) Macrophages express classic netrin-1 receptors UNC5B, Neogenin, and AA2BR. Expression was normalized relative to retinas of normoxic mice at P10. n = 3 independent experiments.

(D) Netrin-1 induced VEGF gene expression in macrophages after 24 hr of incubation with varying doses of netrin-1. Pretreatment with PSB1115 (5 μM) lead to a significant reduction in VEGF expression while anti-UNC5B or anti-neogenin neutralizing antibody (both used at 5 μg/mL) did not affect netrin-1-induced VEGF expression. n = 6 independent experiments. These results were confirmed using siRNA against AA2BR, UNC5B, and neogenin (checkered columns). *p < 0.05, **p < 0.01 relative to vehicle or 100 ng/mL netrin-1 ± SEM. Inset: FACS analysis shows that transfection was effective in macrophages using siGLO reagents (>90% FL-1$^+$ in transfected cells as opposed to <5% FL-1$^+$ in vehicle-transfected controls). Representative of three independent experiments.

(E and F) Netrin-1 (100 ng/mL) induced ERK1/ERK2 phosphorylation in macrophages while pretreatment with PSB1115 (5 μM) blocked the activation of ERK1/ERK2 (depicted at 30 min following stimulation) (F). Representative image of three independent experiments.

to elucidate the mechanism by which ER stress in retinal ganglion neurons stalls neurovascular regeneration, we identified netrin-1 as a selective substrate for IRE1α via a mechanism previously described as IRE1α-dependent decay (RIDD) of messenger RNA (Hollien and Weissman, 2006). Specifically targeting effectors such as netrin-1, while permitting VEGF levels to increase, will hinder netrin-1-induced revascularization while maintaining adequate VEGF levels to provide neurotrophic support of neighboring retinal neural tissue (Robinson et al., 2001). Similarly, it is now believed that several substrates for IRE1α exist including the mRNAs encoding insulin (Lipson et al., 2008), CD59 (Oikawa et al., 2007), HMG-CoA reductase, β2-microglobulin, and the microRNA for TXNIP (miR-17) (Lerner et al., 2012). IRE1α-mediated mRNA degradation provides a rapid mechanism to deplete cells of ER-localized mRNAs and alleviate the metabolic burden of protein folding inside the ER. Interestingly, in our experimental paradigms, we did not observe any direct effects of IRE1α on the induction of VEGF, as has been suggested (Drogat et al., 2007; Ghosh et al., 2010). This could be attributed to IRE1α's ability to adjust its RNase versus transcriptional activity (via activation of XBP1) under conditions of prolonged ER stress (Hollien et al., 2009). In conditions in which homeostasis could not be restored, such as that observed in our experimental paradigms, the RNase activity of IRE1α would be favored over the prosurvival transcriptional induction of angiogenic genes such as VEGF (Han et al., 2009) by IRE1α. Interestingly, as demonstrated in this study, VEGF was found by other reports to be insensitive to the RIDD activity of IRE1α (Ghosh et al., 2010).

Although the nervous system has long been considered immunologically privileged, evidence for direct interplay between the nervous and immune systems is mounting (Farina et al., 2007;

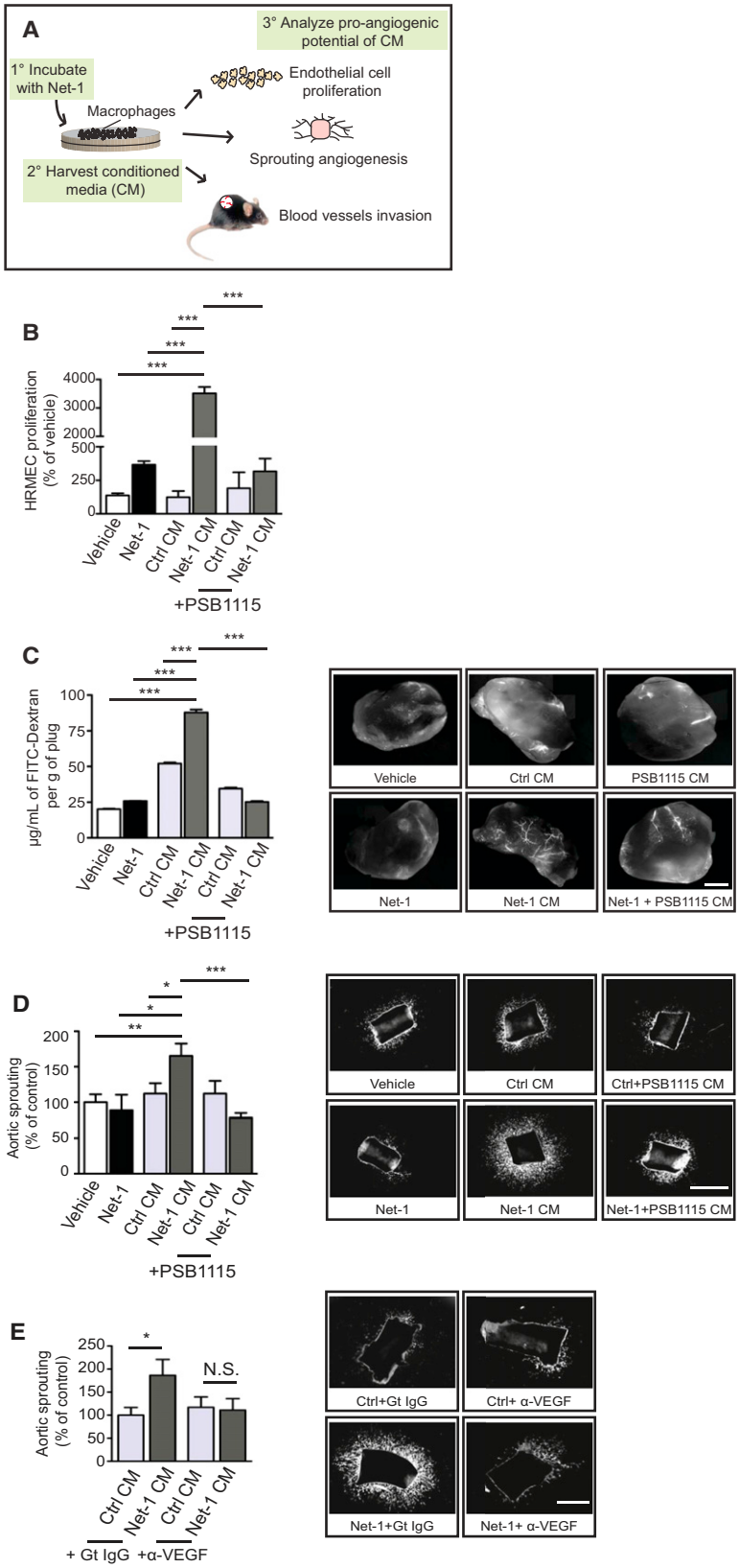

Figure 6. Netrin-1 Triggers a VEGF-Dependent Proangiogenic Response in Macrophages

(A) Schematic description of the experimental design used for assessing the angiogenic potential of macrophage supernatants after netrin-1 challenge.

(B) HRMEC proliferation was assessed by CyQUANT assay after a 48 hr incubation with conditioned media (CM) from macrophages stimulated with vehicle (Ctrl), netrin-1 (100 ng/mL), or netrin-1 stimulation following pretreatment with PSB1115 (5 μM) for 30 min. Cells were incubated in the presence of vehicle (PBS), netrin-1 (100 ng/mL), or macrophage CM. CM from Netrin-1-stimulated macrophages yielded a pronounced increase in cell proliferation in an AA2BR-dependent manner while netrin-1 alone provoked a more modest proliferation (n = 3 separate experiments).

(C) Matrigel plug assay was employed to investigate the ability of macrophage CM to induce vascularization in vivo. CM from same conditions as in (B) were solubilized in Matrigel and implanted in adult mice. Vascular growth inside the subcutaneously injected Matrigel was evaluated by intravenous FITC-dextran injections and spectrophotometric quantification. CM from netrin-1-stimulated macrophages yielded a robust increase in vascular growth in an AA2BR-dependent manner while netrin-1 alone did not influence vascularization. Representative images from Matrigel plugs collected 10 days postintroduction. Scale bar: 2 mm. n = 3 separate experiments.

(D) Area of vascular sprouting from aortic explants incubated with same conditions as in (B). Assessment was made after 48 hr of incubation. Representative images from each condition assessed are shown. n = 12–16 aortic rings from four separate experiments. Scale bar: 1mm.

(E) CM were preincubated with either goat IgG (Gt IgG) or an anti-VEGF neutralizing antibody (5 μg/mL) before addition to aortic explants. Representative images are shown. Scale bar: 1 mm; n = 9–11 aortic rings from three different experiments. *p < 0.05, **p < 0.01, ***p < 0.001 relative to vehicle, netrin-1 100ng/mL, Ctrl CM, or netrin-1 CM ± SEM.

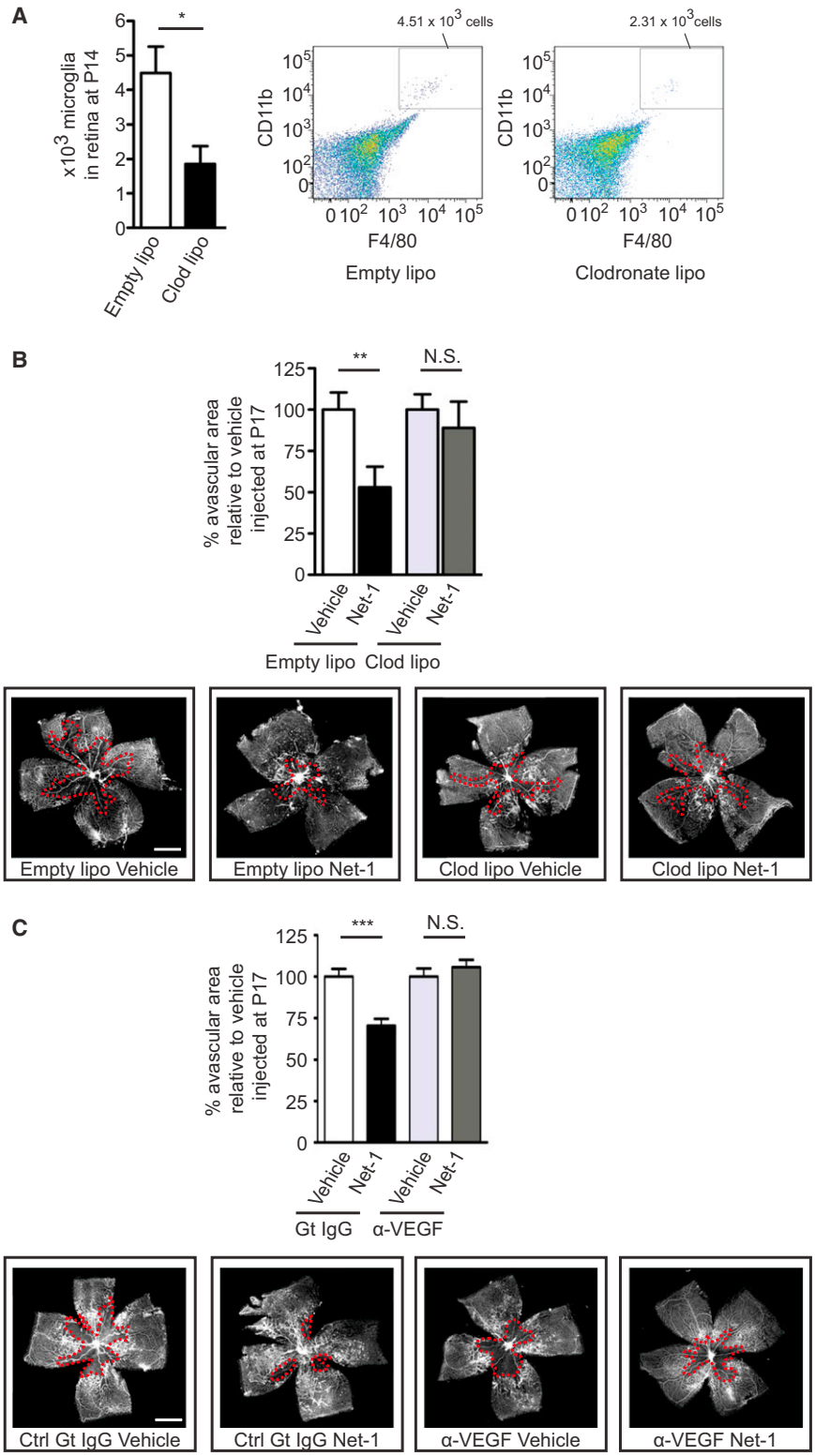

Figure 7. Netrin-1-Dependent Vascular Regeneration Is Macrophage/Microglial Cell and VEGF Dependent

(A) Intravitreal injection of clodronate liposomes efficiently eliminated retinal macrophages/microglia. Retinas were injected at P11 with 1 μL of empty (PBS) or clodronate liposomes and collected at P14 for FACS analysis. The proportion of $CD11b^+/F4\text{-}80^+$ (microglia) was calculated by first gating the 7-AAD negative (viable) population. Histograms showing the numbers of macrophages/microglia according to the proportion measured by FACS analysis. Representative dot plots are shown; n = 6 retinas/group.

(B) Depletion of retinal macrophages abrogated netrin-1-induced revascularization of OIR retinas. Avascular areas were determined in retinas pretreated with 0.5 μL of empty or clodronate-containing liposomes at P11 then injected with 100 ng/mL netrin-1 at P14. Retinas were analyzed at P17. Representative images of flatmount retinas are shown; n = 8–10 animals/group. *p < 0.05, **p < 0.01 relative to vehicle-injected retinas ± SEM. Scale bar: 1 mm.

(C) Simultaneous injections of anti-VEGF neutralizing antibodies at P14 abolished the ability of netrin-1 to induce vascular regeneration. Representative images of n = 8–10 retinal flatmounts per group are shown below. ***p < 0.001 relative to vehicle-injected retinas ± SEM.

(D and E) Graphical depiction of principal findings of the study. Mildly ischemic retinal ganglion neurons produce netrin-1, which activates a critical reparative angiogenic switch in macrophages/microglia and precipitates vascular regeneration of ischemic retinas (D). Sustained hypoxic stress on RGCs provokes the degradation of netrin-1 mRNA by an IRE1α-dependent mechanism and consequently impedes vascular regeneration (E).

London et al., 2011; Nguyen et al., 2002; Rosas-Ballina et al., 2011; Wong et al., 2011). Specifically, the innate immune system has been intimately tied to CNS health and disease. Neuroimmune crosstalk can orchestrate an innate response that participates in beneficial events such as nerve remyelination and microglia-derived neuroprotective trophic support of injured neurons (Nguyen et al., 2002). In the retina, monocyte-derived macrophages participate in promoting RGC survival and nerve regeneration following traumatic optic nerve injury (Leon et al., 2000) as well as neuroprotection against glutamate cytotoxicity and elevated intraocular pressure (London et al., 2011). Of direct pertinence, resident retinal microglia participate actively in promoting developmental vascularization of the ganglion cell layer (Checchin et al., 2006), and resident myeloid cells have the propensity to suppress angiogenic branching (Stefater et al., 2011). Bone marrow-derived myeloid progenitors migrate to avascular areas, differentiate into microglia, and promote revascularization (Ritter et al., 2006). We demonstrate that netrin-1 provokes an angiogenic switch in retinal macrophages and participates in guiding

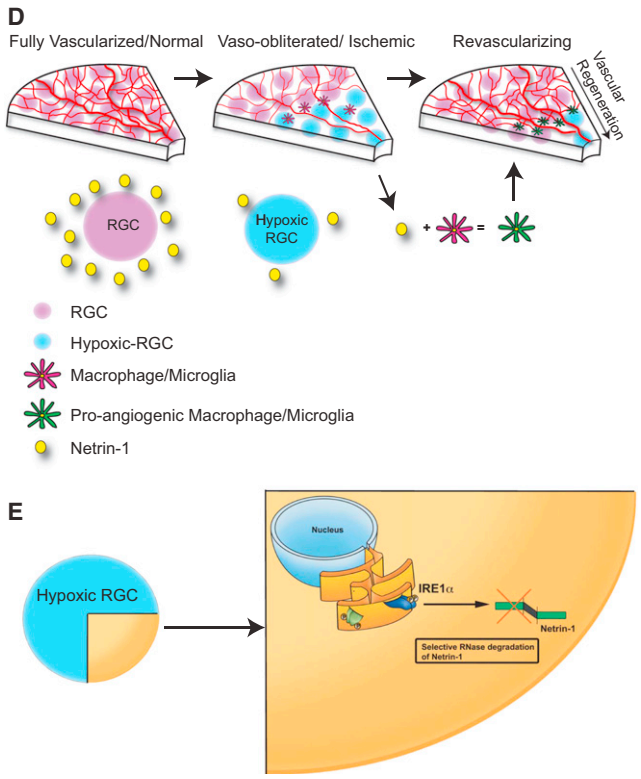

Figure 7. (*continued*).

vascular regrowth into avascular areas of the retina. We show that microglial depletion by clodronate liposomes abolishes the enhanced rate of revascularization induced by netrin-1. In addition, ex vivo and in vitro assays indicate that the proangiogenic effects of netrin-1 are mediated via macrophages in a manner that is dependent on AA2BR function and activation of the ERK1/ERK2 kinase. Hence, the upregulation of VEGF occurs at a microenvironmental level at the vascular front and thus does not precipitate destructive preretinal growth as would be expected by an overall rise in VEGF during the vasoproliferative phase of retinopathy. Interestingly, selective antagonists of the AA2BR were shown to reduce preretinal neovascularization (Mino et al., 2001), suggesting a correlation between this G protein-coupled receptor (GPCR) and retinal angiogenesis. Our data indicate that AA2BR is required for netrin-1 to activate microglia to provide the tissue with an adequate level of VEGF to revascularize the retina without contributing to extraretinal growth. This approach may be considered counterintuitive given the uncontestable involvement of VEGF in the pathogenesis of ocular neovascular disease (Aiello et al., 1995; Caldwell et al., 2003; Ferrara and Kerbel, 2005) and the currently employed anti-angiogenic strategies for proliferative ocular disease (Stewart, 2012). However, providing minute doses of VEGF has been shown to reduce OIR-associated pathology (Dorrell et al., 2010). Consistent with our findings, the ability of physiological doses of netrin-1 (50–200 ng/mL) to promote vascularization and survival of endothelial cells has previously been demonstrated (Park et al., 2004; Wilson et al., 2006). At the same time, however, well-designed and sophisticated studies have described antiangiogenic properties for netrin-1 (Larrivée et al., 2007) acting through the UNC5B receptor (Lu et al., 2004). Our findings indicate that beyond a direct effect on endothelium, netrin-1 influences cell populations associated with the vasculature and suggest that this may account for some of the noted discrepancies (Castets and Mehlen, 2010). It is important to note that although it has been suggested that AA2BR functions as a receptor for netrin-1 (Corset et al., 2000; Mirakaj et al., 2011; Rosenberger et al., 2009), these results have been controversial (Stein et al., 2001). Alternatively, manipulating AA2BR function directly regulates the intracellular concentration of cyclic AMP (cAMP), which in neurons regulates the switch between chemoattractant and chemorepellent responses to a netrin-1 gradient (Nishiyama et al., 2003; Shewan et al., 2002). We speculate that a similar paradigm may thus apply to macrophages, with intracellular levels of cAMP potentiating the angiogenic switch.

Collectively, these findings provide mechanistic insight into vascular regeneration in neuroischemic conditions. Our data present the ER of CNS neurons as a key sensor of hypoxic stress that has the propensity to modulate the reparative innate immune response under ischemic conditions. In doing so, we provide evidence for neuroimmune communication in neuroischemic conditions such as proliferative retinopathies. When driven beyond a hypoxic threshold however, central neurons via IRE1α have the ability to halt vascularization, possibly in order to deviate metabolic stores to more salvageable areas. To date, there are no therapeutic strategies that aim to enhance vascular regeneration in ischemic CNS tissue. In this regard, netrin-1-stimulated macrophages may be able to override the vasoinhibitory cues present within the ischemic neuronal retina (Fukushima et al., 2011; Joyal et al., 2011) and achieve functional vascular regeneration. The work presented in this study provides proof of concept for the modulation of ER stress and netrin-1 for an ischemic disorder of the CNS. Future investigation and streamlining will be required to translate these findings and design therapeutic strategies to counter neuroischemic conditions such as retinopathies.

EXPERIMENTAL PROCEDURES

Animals

All studies were performed according to the Association for Research in Vision and Ophthalmology (ARVO) Statement for the Use of Animals in Ophthalmic and Vision Research and were approved by the Animal Care Committee of the University of Montreal in agreement with the guidelines established by the Canadian Council on Animal Care. C57Bl/6 wild-type were purchased from The Jackson Laboratory and CD1 nursing mothers from Charles River Laboratories.

Depletion of Macrophages by Clodronate Liposomes

We prepared clodronate liposomes (0.7 M) or control empty-liposomes (PBS-filled) as described (van Rooijen and van Kesteren-Hendrikx, 2003) and delivered them by intravitreal injection (0.5 μL) at P11. To visualize and ascertain uptake of liposomes in macrophages in vitro and in vivo, we incubated liposomes with the fluorescent lipophilic marker DiI according to the manufacturer's protocol (Invitrogen).

O_2-Induced Retinopathy

Mouse pups (C57Bl6; The Jackson Laboratory) and their fostering mothers (CD1; Charles River Laboratories) were exposed to 75% O_2 from P7–P12 and returned to room air. This model serves as a proxy to human ocular

neovascular diseases such as ROP and diabetic retinopathy characterized by a late phase of destructive pathological angiogenesis (Sapieha, 2012; Stahl et al., 2010). Upon return to room air, hypoxia-driven neovascularization (NV) develops from P14 onward (Smith et al., 1994). We enucleated eyes at different time points and dissected the retinas for mRNA or protein assays as described. Dissected retinas were flatmounted and incubated overnight with fluoresceinated isolectin B4 (1:100) in 1 mM $CaCl_2$ to determine the extent of avascular area or neovascularization area at P17 using ImageJ and the SWIFT-NV method (Stahl et al., 2009).

Semiquantitative and Real-Time PCR Analysis

We isolated RNA using the GenElute Mammalian Total RNA Miniprep Kit (Sigma-Aldrich) and performed a digestion with deoxyribonuclease I (DNase I) to prevent amplification of genomic DNA. We reverse transcribed the RNA using M-MLV reverse transcriptase and analyzed gene expression using Sybr Green in an ABI real-time PCR machine (Applied Biosystems). β-actin was used as a reference gene. Primers sequences are displayed in Figure S7. We investigated the splicing of XBP1 by incubating the XBP1 semiquantitative PCR product with 0.4 U/μL of PstI enzyme for 5 hr at 37°C followed by separation on 2.5% agarose gel.

Laser-Capture Microdissection

Eyes were enucleated from P14 pups in OIR or normoxic littermates and flash frozen in OCT. We then cut 12 μm sections using a Leica cryostat at −20°C and air dried for 10 min. We dissected retinal layers using a Zeiss Observer microscope equipped with a PALM MicroBeam device for laser capture microdissection. We isolated mRNA from these sections and performed qPCRs as described above.

Western Blotting

For assessment of retinal protein levels, we enucleated eyes at varying time points and rapidly dissected and homogenized retinas. Protein concentrations were assessed by BCA assay (Sigma), and then 30 ug of protein was analyzed for each condition by standard SDS-PAGE technique. Antibodies used for western blotting are listed in Figure S7.

Immunohistochemistry

To localize protein expression, eyes were enucleated from mice and fixed in 4% paraformaldehyde at room temperature for 4 hr, incubated in 30% sucrose overnight, and then frozen in OCT compound. We then embedded the whole eye in optimal cutting temperature compound at −20°C and performed 12 μm serial sections. We carried out immunohistochemistry experiments and visualized the sections with an epifluorescent microscope (Zeiss Axio Imager). Antibodies used for immunohistochemistry are listed in Figure S7. For visualization of panretinal vasculature, flatmount retinas were stained with fluoresceinated Isolectin B4 (Alexa Fluor 594 [I21413]; Molecular Probes) in 1 mM $CaCl_2$ in PBS for retinal vasculature. For assessment of vascular permeability, we injected the mice intracardially with 10 mg/mL of 70 kDa FITC-dextran. After 5 min, the eyes were harvested and retinas were dissected for flatmouting and visualization under a fluorescent microscope.

Preparation of Lentivirus

We produced infectious lentiviral vectors by transfecting lentivector and packaging vectors into HEK293T cells (Invitrogen) as previously described (Dull et al., 1998). Viral supernatants were concentrated by ultracentrifugation (>500-fold) and titers determined by ELISA for viral p24 antigen using a commercial kit (Clontech). The titers of the lentiviruses used were (in ng p24) LV.GFP (15.0 ng/μL), LV.sh.RNA IRE1α (8.52 ng/μL), and LV.sh.RNA.GFP (8.47 ng/μL).

Generation of Stable PERK- and IRE1α-Deficient RGC-5 Cell Lines and Transfections

We stably transfected RGC-5 cells with 500 ng of shRNA plasmids targeting PERK or IRE1α (Open Biosystems) or an unrelated shRNA (shGFP) for 16 hr at 37°C using Lipofectamine 2000 following the manufacturer's directions. We generated stable cell lines by selecting with 2 μg of puromycin over 2 weeks. For analysis of cleavage of netrin-1, we transfected 1 μg of an expression plasmid for chicken netrin-1 with or without the expression plasmids for shGFP, IRE1α or a dominant-negative mutant of IREα K599A, or the RNase dead mutant K907A in HEK293T cells using Lipofectamine 2000. Plasmids for IRE1α and IRE1α K599A were a gift from Fumihiko Urano (Addgene plasmid #20744 and #20745), and plasmid K907A was kindly provided by Randal J. Kaufman (Sanford-Burnham Medical Research Institute).

Detection of Intravitreally Delivered Netrin-1

We injected a recombinant Myc-tagged netrin-1 protein in P14 OIR animals. We collected eyes 3 hr later then fixed and dissected the retinas. We stained the retinas using a Myc antibody, Iba1, and fluoresceinated isolectin B4. Flatmounted retinas were visualized using a confocal microscope equipped with an argon laser (LMS5; Zeiss). We generated a 3D reconstruction of >20 z stack layers using the Velocity software.

Microvascular Sprouting of Aortic Rings

Aortae from adult C57Bl6 mice were dissected and sectioned into 1 mm rings, which were immediately transferred to reduced growth factor Matrigel. After 3 days in EBM basal medium (Lonza), we incubated the rings with 500 uL of macrophage-conditioned media. Rings were photographed with an inverted microscope (Zeiss Axio Imager) before and 48 hr posttreatment. Variation in the vascular area surrounding the aortic ring was calculated using ImageJ software.

CyQUANT Proliferation Assay

Primary human retinal microvascular endothelial cells (HRMEC passages six to ten from Cell Systems) were starved for 12 hr in EBM-2 medium (Lonza) plus 0.5% fetal bovine serum prior to treatment with macrophage-conditioned media or controls. We assessed the proliferation rates of 5,000 HRMEC cells/well using the CyQUANT NF Cell Proliferation Assay Kit (Invitrogen) (according to instructions given by the manufacturer) after 48 hr of incubation.

Isolation of Primary Microglia

Brains from P14 pups were homogenized in ice-cold L15 medium (GIBCO) and incubated for 15 min in 0.05% trypsin-EDTA (GIBCO) at 37°C. The reaction was stopped by addition of equal volumes of fetal bovine serum. We added 75 U/mL of DNase I (Sigma) before filtering through a 70 μm cell strainer. After 9 days of incubation in DMEM media (Invitrogen) supplemented with 10% fetal bovine serum and penicillin/streptomycin, microglia were detached from the plates by gentle shaking (150 rpm for 2 hr at 37°C). Purity of preparations was confirmed by FACS analysis.

Matrigel Plug Assay

Macrophage-conditioned media (80 μl) was mixed with 500 uL of reduced growth factor Matrigel (BD Biosciences) at 4°C. The mixture was injected subcutaneously in the abdominal region of C57Bl6 mice (6 weeks old). After 10 days, we injected 200 μl of FITC-dextran (2,000,000 MW; 25 mg/mL) intravenously 15 min prior to dissection of the overlying skin and harvesting of the Matrigel plug. We photographed the plugs using an epifluorescent microscope (Zeiss AxioImager) then weighted and homogenized the plugs in 1 mg/mL of collagenase/dispase (Roche) overnight at 37°C in the dark. The next day, we centrifuged homogenates and measured fluorescence intensity of supernatants at 480/520 nm.

FACS of Digested Retinas

Retinas from clodronate or empty liposome-injected eyes were homogenized with a solution of 750 U/mL DNaseI (Sigma) and 0.5 mg/mL of collagenase D (Roche) for 15 min at 37°C with gentle shaking. Homogenates were the filtered with a 70 μm cell strainer and washed in RPMI + 2% fetal bovine serum. We used PE-F4/80, FITC-CD11b, 7-AAD antibodies for detection of macrophages and performed analysis using a BD FACSCanto device (BD Biosciences) and the FlowJo 7.6 software. Antibodies are listed in Figure S7.

Preparation of Macrophage-Conditioned Media

Supernatants were collected from J774 cells that had been incubated for 24 hr in the presence of various concentrations of netrin-1 and/or inhibitors. Supernatants were centrifuged, filtered, and then frozen for subsequent use.

Secondary Structure Reconstruction of Netrin-1 mRNA

For prediction of the secondary structure of mRNA, we analyzed the murine sequence of netrin-1 mRNA using CentroidFold program (http://www.ncrna.org/centroidfold).

IRE1α In Vitro Cleavage Assay

Thirty micrograms of total RNA extracted from HEK transfected or not with an expression plasmid for netrin-1 was subjected to digestion by the IRE1α recombinant enzyme (5 μg) for 2 hr at 37°C in a 5× digestion buffer (250 mM Tris [pH 7.5], 600 mM NaCl, 5 mM $MgCl_2$, 5 mM $MnCl_2$, 25 mM β-mercaptoethanol, 10 mM ATP). The digested RNA was analyzed by semi-quantitative PCR using sets of primers spanning different regions in the netrin-1 mRNA.

Northern Blotting

Fifty micrograms of total RNA was separated on a formaldehyde agarose gel and transferred to a nitrocellulose membrane. The membrane was then incubated with a radiolabelled netrin-1-specific probe (<500 pb fragment of a SacII-PvuI digestion product of the netrin-1 expression plasmid) overnight at 42°C.

Statistical Analyses

Data are presented as mean ± SEM. We used Student's t test to compare the different groups; $p < 0.05$ was considered statistically different.

SUPPLEMENTAL INFORMATION

Supplemental Information includes seven figures and one movie and can be found with this article online at http://dx.doi.org/10.1016/j.cmet.2013.02.003.

ACKNOWLEDGMENTS

This work was supported by operating grants to P.S. from the Canadian Institutes of Health Research (221478), the Canadian Diabetes Association (OG-3-11-3329-PS), and the Natural Sciences and Engineering Research Council of Canada (418637). P.S. holds a Canada Research Chair in Retinal Cell Biology and The Alcon Research Institute Young Investigator Award. F.B. holds a Fonds de la recherche en santé du Québec (FRSQ) postdoctoral fellowship. G.M. and A.C. are supported by scholarships from the Réseau de Recherche en Santé de la Vision du Québec. N.S. holds an FRSQ doctoral scholarship. T.E.K. holds an FRSQ Chercheurs Nationaux award and is a Killam Foundation Scholar. NIH grants R37DK042394, R01DK088227, P01HL057346R01, and R01HL052173 were awarded to R.J.K. We would like to thank Isabelle Louarn for the artwork in Figure 1. We thank Dr. Jing Chen for critical comments on the manuscript. We also wish to acknowledge Vincent Bourgoin, Stefania Bottardi, and Vincent Lemay for technical advices. F.B., N.T., M.G., T.E.K., and P.S. conceived and designed the experiments; F.B., G.M., N.S., N.T., S.F., E.L., A.C., D.L., S.T., F.R., A.M.J., and J.-S.J. performed the experiments; F.B. and P.S. analyzed the data; A.S., E.M., R.K., and M.G. provided expert advice; and P.S., F.B., and T.E.K. wrote the paper.

Received: April 25, 2012
Revised: October 26, 2012
Accepted: January 23, 2013
Published: March 5, 2013

REFERENCES

Adams, R.H., and Eichmann, A. (2010). Axon guidance molecules in vascular patterning. Cold Spring Harb. Perspect. Biol. *2*, a001875.

Adams, R.H., Wilkinson, G.A., Weiss, C., Diella, F., Gale, N.W., Deutsch, U., Risau, W., and Klein, R. (1999). Roles of ephrinB ligands and EphB receptors in cardiovascular development: demarcation of arterial/venous domains, vascular morphogenesis, and sprouting angiogenesis. Genes Dev. *13*, 295–306.

Aiello, L.P. (2005). Angiogenic pathways in diabetic retinopathy. N. Engl. J. Med. *353*, 839–841.

Aiello, L.P., Pierce, E.A., Foley, E.D., Takagi, H., Chen, H., Riddle, L., Ferrara, N., King, G.L., and Smith, L.E. (1995). Suppression of retinal neovascularization in vivo by inhibition of vascular endothelial growth factor (VEGF) using soluble VEGF-receptor chimeric proteins. Proc. Natl. Acad. Sci. USA *92*, 10457–10461.

Ashton, N., Ward, B., and Serpell, G. (1954). Effect of oxygen on developing retinal vessels with particular reference to the problem of retrolental fibroplasia. Br. J. Ophthalmol. *38*, 397–432.

Bernales, S., Papa, F.R., and Walter, P. (2006). Intracellular signaling by the unfolded protein response. Annu. Rev. Cell Dev. Biol. *22*, 487–508.

Bruick, R.K. (2003). Oxygen sensing in the hypoxic response pathway: regulation of the hypoxia-inducible transcription factor. Genes Dev. *17*, 2614–2623.

Caldwell, R.B., Bartoli, M., Behzadian, M.A., El-Remessy, A.E., Al-Shabrawey, M., Platt, D.H., and Caldwell, R.W. (2003). Vascular endothelial growth factor and diabetic retinopathy: pathophysiological mechanisms and treatment perspectives. Diabetes Metab. Res. Rev. *19*, 442–455.

Campbell, K. (1951). Intensive oxygen therapy as a possible cause of retrolental fibroplasia; a clinical approach. Med. J. Aust. *2*, 48–50.

Carmeliet, P., and Jain, R.K. (2011). Molecular mechanisms and clinical applications of angiogenesis. Nature *473*, 298–307.

Carmeliet, P., and Tessier-Lavigne, M. (2005). Common mechanisms of nerve and blood vessel wiring. Nature *436*, 193–200.

Castets, M., and Mehlen, P. (2010). Netrin-1 role in angiogenesis: to be or not to be a pro-angiogenic factor? Cell Cycle *9*, 1466–1471.

Checchin, D., Sennlaub, F., Levavasseur, E., Leduc, M., and Chemtob, S. (2006). Potential role of microglia in retinal blood vessel formation. Invest. Ophthalmol. Vis. Sci. *47*, 3595–3602.

Chen, J., and Smith, L.E. (2007). Retinopathy of prematurity. Angiogenesis *10*, 133–140.

Chen, X., Kintner, D.B., Luo, J., Baba, A., Matsuda, T., and Sun, D. (2008). Endoplasmic reticulum Ca2+ dysregulation and endoplasmic reticulum stress following in vitro neuronal ischemia: role of Na+-K+-Cl- cotransporter. J. Neurochem. *106*, 1563–1576.

Cheung, N., and Wong, T.Y. (2008). Diabetic retinopathy and systemic vascular complications. Prog. Retin. Eye Res. *27*, 161–176.

Corset, V., Nguyen-Ba-Charvet, K.T., Forcet, C., Moyse, E., Chédotal, A., and Mehlen, P. (2000). Netrin-1-mediated axon outgrowth and cAMP production requires interaction with adenosine A2b receptor. Nature *407*, 747–750.

D'Amore, P.A., and Sweet, E. (1987). Effects of hyperoxia on microvascular cells in vitro. In Vitro Cell. Dev. Biol. *23*, 123–128.

Dorrell, M.I., and Friedlander, M. (2006). Mechanisms of endothelial cell guidance and vascular patterning in the developing mouse retina. Prog. Retin. Eye Res. *25*, 277–295.

Dorrell, M.I., Aguilar, E., Jacobson, R., Trauger, S.A., Friedlander, J., Siuzdak, G., and Friedlander, M. (2010). Maintaining retinal astrocytes normalizes revascularization and prevents vascular pathology associated with oxygen-induced retinopathy. Glia *58*, 43–54.

Drogat, B., Auguste, P., Nguyen, D.T., Bouchecareilh, M., Pineau, R., Nalbantoglu, J., Kaufman, R.J., Chevet, E., Bikfalvi, A., and Moenner, M. (2007). IRE1 signaling is essential for ischemia-induced vascular endothelial growth factor-A expression and contributes to angiogenesis and tumor growth in vivo. Cancer Res. *67*, 6700–6707.

Dull, T., Zufferey, R., Kelly, M., Mandel, R.J., Nguyen, M., Trono, D., and Naldini, L. (1998). A third-generation lentivirus vector with a conditional packaging system. J. Virol. *72*, 8463–8471.

Edwards, M.M., McLeod, D.S., Li, R., Grebe, R., Bhutto, I., Mu, X., and Lutty, G.A. (2012). The deletion of Math5 disrupts retinal blood vessel and glial development in mice. Exp. Eye Res. *96*, 147–156.

Eichmann, A., and Thomas, J.L. (2012). Molecular Parallels between Neural and Vascular Development (New York: Cold Spring Harb Perspect Med).

Erskine, L., Reijntjes, S., Pratt, T., Denti, L., Schwarz, Q., Vieira, J.M., Alakakone, B., Shewan, D., and Ruhrberg, C. (2011). VEGF signaling through neuropilin 1 guides commissural axon crossing at the optic chiasm. Neuron *70*, 951–965.

Fantin, A., Vieira, J.M., Gestri, G., Denti, L., Schwarz, Q., Prykhozhij, S., Peri, F., Wilson, S.W., and Ruhrberg, C. (2010). Tissue macrophages act as cellular chaperones for vascular anastomosis downstream of VEGF-mediated endothelial tip cell induction. Blood *116*, 829–840.

Farina, C., Aloisi, F., and Meinl, E. (2007). Astrocytes are active players in cerebral innate immunity. Trends Immunol. *28*, 138–145.

Ferrara, N., and Kerbel, R.S. (2005). Angiogenesis as a therapeutic target. Nature *438*, 967–974.

Fujita, H., Zhang, B., Sato, K., Tanaka, J., and Sakanaka, M. (2001). Expressions of neuropilin-1, neuropilin-2 and semaphorin 3A mRNA in the rat brain after middle cerebral artery occlusion. Brain Res. *914*, 1–14.

Fukushima, Y., Okada, M., Kataoka, H., Hirashima, M., Yoshida, Y., Mann, F., Gomi, F., Nishida, K., Nishikawa, S., and Uemura, A. (2011). Sema3E-PlexinD1 signaling selectively suppresses disoriented angiogenesis in ischemic retinopathy in mice. J. Clin. Invest. *121*, 1974–1985.

Gerhardt, H., Golding, M., Fruttiger, M., Ruhrberg, C., Lundkvist, A., Abramsson, A., Jeltsch, M., Mitchell, C., Alitalo, K., Shima, D., and Betsholtz, C. (2003). VEGF guides angiogenic sprouting utilizing endothelial tip cell filopodia. J. Cell Biol. *161*, 1163–1177.

Ghosh, R., Lipson, K.L., Sargent, K.E., Mercurio, A.M., Hunt, J.S., Ron, D., and Urano, F. (2010). Transcriptional regulation of VEGF-A by the unfolded protein response pathway. PLoS ONE *5*, e9575.

Gilbert, C., Rahi, J., Eckstein, M., O'Sullivan, J., and Foster, A. (1997). Retinopathy of prematurity in middle-income countries. Lancet *350*, 12–14.

Han, D., Lerner, A.G., Vande Walle, L., Upton, J.-P., Xu, W., Hagen, A., Backes, B.J., Oakes, S.A., and Papa, F.R. (2009). IRE1alpha kinase activation modes control alternate endoribonuclease outputs to determine divergent cell fates. Cell *138*, 562–575.

Hayashi, T., Saito, A., Okuno, S., Ferrand-Drake, M., Dodd, R.L., and Chan, P.H. (2005). Damage to the endoplasmic reticulum and activation of apoptotic machinery by oxidative stress in ischemic neurons. J. Cereb. Blood Flow Metab. *25*, 41–53.

Hollien, J., and Weissman, J.S. (2006). Decay of endoplasmic reticulum-localized mRNAs during the unfolded protein response. Science *313*, 104–107.

Hollien, J., Lin, J.H., Li, H., Stevens, N., Walter, P., and Weissman, J.S. (2009). Regulated Ire1-dependent decay of messenger RNAs in mammalian cells. J. Cell Biol. *186*, 323–331.

Ishida, S., Usui, T., Yamashiro, K., Kaji, Y., Amano, S., Ogura, Y., Hida, T., Oguchi, Y., Ambati, J., Miller, J.W., et al. (2003). VEGF164-mediated inflammation is required for pathological, but not physiological, ischemia-induced retinal neovascularization. J. Exp. Med. *198*, 483–489.

Jones, C.A., London, N.R., Chen, H., Park, K.W., Sauvaget, D., Stockton, R.A., Wythe, J.D., Suh, W., Larrieu-Lahargue, F., Mukouyama, Y.S., et al. (2008). Robo4 stabilizes the vascular network by inhibiting pathologic angiogenesis and endothelial hyperpermeability. Nat. Med. *14*, 448–453.

Joyal, J.-S., Sitaras, N., Binet, F., Rivera, J.C., Stahl, A., Zaniolo, K., Shao, Z., Polosa, A., Zhu, T., Hamel, D., et al. (2011). Ischemic neurons prevent vascular regeneration of neural tissue by secreting semaphorin 3A. Blood *117*, 6024–6035.

Kempen, J.H., O'Colmain, B.J., Leske, M.C., Haffner, S.M., Klein, R., Moss, S.E., Taylor, H.R., and Hamman, R.F.; Eye Diseases Prevalence Research Group. (2004). The prevalence of diabetic retinopathy among adults in the United States. Arch. Ophthalmol. *122*, 552–563.

Kennedy, T.E., Serafini, T., de la Torre, J.R., and Tessier-Lavigne, M. (1994). Netrins are diffusible chemotropic factors for commissural axons in the embryonic spinal cord. Cell *78*, 425–435.

Kim, J., Oh, W.J., Gaiano, N., Yoshida, Y., and Gu, C. (2011). Semaphorin 3E-Plexin-D1 signaling regulates VEGF function in developmental angiogenesis via a feedback mechanism. Genes Dev. *25*, 1399–1411.

Klagsbrun, M., and Eichmann, A. (2005). A role for axon guidance receptors and ligands in blood vessel development and tumor angiogenesis. Cytokine Growth Factor Rev. *16*, 535–548.

Lang, R.A., and Bishop, J.M. (1993). Macrophages are required for cell death and tissue remodeling in the developing mouse eye. Cell *74*, 453–462.

Lange, C.A., and Bainbridge, J.W. (2012). Oxygen sensing in retinal health and disease. Ophthalmologica *227*, 115–131.

Lange, C.A., Stavrakas, P., Luhmann, U.F., de Silva, D.J., Ali, R.R., Gregor, Z.J., and Bainbridge, J.W. (2011). Intraocular oxygen distribution in advanced proliferative diabetic retinopathy. Am. J. Ophthalmol. *152*, 406–412, e3.

Larrivée, B., Freitas, C., Trombe, M., Lv, X., Delafarge, B., Yuan, L., Bouvrée, K., Bréant, C., Del Toro, R., Bréchot, N., et al. (2007). Activation of the UNC5B receptor by Netrin-1 inhibits sprouting angiogenesis. Genes Dev. *21*, 2433–2447.

Larrivée, B., Freitas, C., Suchting, S., Brunet, I., and Eichmann, A. (2009). Guidance of vascular development: lessons from the nervous system. Circ. Res. *104*, 428–441.

Lee, J., Sun, C., Zhou, Y., Lee, J., Gokalp, D., Herrema, H., Park, S.W., Davis, R.J., and Ozcan, U. (2011). p38 MAPK-mediated regulation of Xbp1s is crucial for glucose homeostasis. Nat. Med. *17*, 1251–1260.

Lejmi, E., Leconte, L., Pédron-Mazoyer, S., Ropert, S., Raoul, W., Lavalette, S., Bouras, I., Feron, J.G., Maitre-Boube, M., Assayag, F., et al. (2008). Netrin-4 inhibits angiogenesis via binding to neogenin and recruitment of Unc5B. Proc. Natl. Acad. Sci. USA *105*, 12491–12496.

Leon, S., Yin, Y., Nguyen, J., Irwin, N., and Benowitz, L.I. (2000). Lens injury stimulates axon regeneration in the mature rat optic nerve. J. Neurosci. *20*, 4615–4626.

Lerner, A.G., Upton, J.P., Praveen, P.V., Ghosh, R., Nakagawa, Y., Igbaria, A., Shen, S., Nguyen, V., Backes, B.J., Heiman, M., et al. (2012). IRE1α induces thioredoxin-interacting protein to activate the NLRP3 inflammasome and promote programmed cell death under irremediable ER stress. Cell Metab. *16*, 250–264.

Lipson, K.L., Ghosh, R., and Urano, F. (2008). The role of IRE1alpha in the degradation of insulin mRNA in pancreatic beta-cells. PLoS ONE *3*, e1648.

Lo, E.H. (2008). A new penumbra: transitioning from injury into repair after stroke. Nat. Med. *14*, 497–500.

London, A., Itskovich, E., Benhar, I., Kalchenko, V., Mack, M., Jung, S., and Schwartz, M. (2011). Neuroprotection and progenitor cell renewal in the injured adult murine retina requires healing monocyte-derived macrophages. J. Exp. Med. *208*, 23–39.

Lu, X., Le Noble, F., Yuan, L., Jiang, Q., De Lafarge, B., Sugiyama, D., Bréant, C., Claes, F., De Smet, F., Thomas, J.L., et al. (2004). The netrin receptor UNC5B mediates guidance events controlling morphogenesis of the vascular system. Nature *432*, 179–186.

Lundbaek, K., Christensen, N.J., Jensen, V.A., Johansen, K., Olsen, T.S., Hansen, A.P., Orskov, H., and Osterby, R. (1970). Diabetes, diabetic angiopathy, and growth hormone. Lancet *2*, 131–133.

Ly, N.P., Komatsuzaki, K., Fraser, I.P., Tseng, A.A., Prodhan, P., Moore, K.J., and Kinane, T.B. (2005). Netrin-1 inhibits leukocyte migration in vitro and in vivo. Proc. Natl. Acad. Sci. USA *102*, 14729–14734.

Malhi, H., and Kaufman, R.J. (2011). Endoplasmic reticulum stress in liver disease. J. Hepatol. *54*, 795–809.

Marciniak, S.J., and Ron, D. (2006). Endoplasmic reticulum stress signaling in disease. Physiol. Rev. *86*, 1133–1149.

Miao, H.Q., Soker, S., Feiner, L., Alonso, J.L., Raper, J.A., and Klagsbrun, M. (1999). Neuropilin-1 mediates collapsin-1/semaphorin III inhibition of endothelial cell motility: functional competition of collapsin-1 and vascular endothelial growth factor-165. J. Cell Biol. *146*, 233–242.

Michaelson, I.C. (1948). The mode of development of the vascular system of the retina with some observations on its significance for certain retinal disorders. Trans. Ophthalmol. Soc. UK. *68*, 137–180.

Mino, R.P., Spoerri, P.E., Caballero, S., Player, D., Belardinelli, L., Biaggioni, I., and Grant, M.B. (2001). Adenosine receptor antagonists and retinal neovascularization in vivo. Invest. Ophthalmol. Vis. Sci. *42*, 3320–3324.

Mirakaj, V., Gatidou, D., Pötzsch, C., König, K., and Rosenberger, P. (2011). Netrin-1 signaling dampens inflammatory peritonitis. J. Immunol. *186*, 549–555.

Moskowitz, M.A., Lo, E.H., and Iadecola, C. (2010). The science of stroke: mechanisms in search of treatments. Neuron *67*, 181–198.

Nguyen, M.D., Julien, J.P., and Rivest, S. (2002). Innate immunity: the missing link in neuroprotection and neurodegeneration? Nat. Rev. Neurosci. *3*, 216–227.

Nishiyama, M., Hoshino, A., Tsai, L., Henley, J.R., Goshima, Y., Tessier-Lavigne, M., Poo, M.M., and Hong, K. (2003). Cyclic AMP/GMP-dependent modulation of Ca2+ channels sets the polarity of nerve growth-cone turning. Nature *423*, 990–995.

Oikawa, D., Tokuda, M., and Iwawaki, T. (2007). Site-specific cleavage of CD59 mRNA by endoplasmic reticulum-localized ribonuclease, IRE1. Biochem. Biophys. Res. Commun. *360*, 122–127.

Oikawa, D., Tokuda, M., Hosoda, A., and Iwawaki, T. (2010). Identification of a consensus element recognized and cleaved by IRE1 alpha. Nucleic Acids Res. *38*, 6265–6273.

Oyadomari, S., and Mori, M. (2004). Roles of CHOP/GADD153 in endoplasmic reticulum stress. Cell Death Differ. *11*, 381–389.

Park, K.W., Crouse, D., Lee, M., Karnik, S.K., Sorensen, L.K., Murphy, K.J., Kuo, C.J., and Li, D.Y. (2004). The axonal attractant Netrin-1 is an angiogenic factor. Proc. Natl. Acad. Sci. USA *101*, 16210–16215.

Paschen, W., and Doutheil, J. (1999). Disturbances of the functioning of endoplasmic reticulum: a key mechanism underlying neuronal cell injury? J. Cereb. Blood Flow Metab. *19*, 1–18.

Paul, S.A., Simons, J.W., and Mabjeesh, N.J. (2004). HIF at the crossroads between ischemia and carcinogenesis. J. Cell. Physiol. *200*, 20–30.

Pierce, E.A., Avery, R.L., Foley, E.D., Aiello, L.P., and Smith, L.E. (1995). Vascular endothelial growth factor/vascular permeability factor expression in a mouse model of retinal neovascularization. Proc. Natl. Acad. Sci. USA *92*, 905–909.

Pierce, E.A., Foley, E.D., and Smith, L.E. (1996). Regulation of vascular endothelial growth factor by oxygen in a model of retinopathy of prematurity. Arch. Ophthalmol. *114*, 1219–1228.

Ritter, M.R., Banin, E., Moreno, S.K., Aguilar, E., Dorrell, M.I., and Friedlander, M. (2006). Myeloid progenitors differentiate into microglia and promote vascular repair in a model of ischemic retinopathy. J. Clin. Invest. *116*, 3266–3276.

Robinson, G.S., Ju, M., Shih, S.C., Xu, X., McMahon, G., Caldwell, R.B., and Smith, L.E. (2001). Nonvascular role for VEGF: VEGFR-1, 2 activity is critical for neural retinal development. FASEB J. *15*, 1215–1217.

Ron, D., and Walter, P. (2007). Signal integration in the endoplasmic reticulum unfolded protein response. Nat. Rev. Mol. Cell Biol. *8*, 519–529.

Rosas-Ballina, M., Olofsson, P.S., Ochani, M., Valdés-Ferrer, S.I., Levine, Y.A., Reardon, C., Tusche, M.W., Pavlov, V.A., Andersson, U., Chavan, S., et al. (2011). Acetylcholine-synthesizing T cells relay neural signals in a vagus nerve circuit. Science *334*, 98–101.

Rosenberger, P., Schwab, J.M., Mirakaj, V., Masekowsky, E., Mager, A., Morote-Garcia, J.C., Unertl, K., and Eltzschig, H.K. (2009). Hypoxia-inducible factor-dependent induction of netrin-1 dampens inflammation caused by hypoxia. Nat. Immunol. *10*, 195–202.

Sapieha, P. (2012). Eyeing central neurons in vascular growth and reparative angiogenesis. Blood *120*, 2182–2194.

Sapieha, P., Sirinyan, M., Hamel, D., Zaniolo, K., Joyal, J.-S., Cho, J.-H., Honoré, J.-C., Kermorvant-Duchemin, E., Varma, D.R., Tremblay, S., et al. (2008). The succinate receptor GPR91 in neurons has a major role in retinal angiogenesis. Nat. Med. *14*, 1067–1076.

Sapieha, P., Hamel, D., Shao, Z., Rivera, J.C., Zaniolo, K., Joyal, J.S., and Chemtob, S. (2010a). Proliferative retinopathies: angiogenesis that blinds. Int. J. Biochem. Cell Biol. *42*, 5–12.

Sapieha, P., Joyal, J.S., Rivera, J.C., Kermorvant-Duchemin, E., Sennlaub, F., Hardy, P., Lachapelle, P., and Chemtob, S. (2010b). Retinopathy of prematurity: understanding ischemic retinal vasculopathies at an extreme of life. J. Clin. Invest. *120*, 3022–3032.

Schröder, M., and Kaufman, R.J. (2005). ER stress and the unfolded protein response. Mutat. Res. *569*, 29–63.

Shekarabi, M., and Kennedy, T.E. (2002). The netrin-1 receptor DCC promotes filopodia formation and cell spreading by activating Cdc42 and Rac1. Mol. Cell. Neurosci. *19*, 1–17.

Shewan, D., Dwivedy, A., Anderson, R., and Holt, C.E. (2002). Age-related changes underlie switch in netrin-1 responsiveness as growth cones advance along visual pathway. Nat. Neurosci. *5*, 955–962.

Simons, B.D., and Flynn, J.T. (1999). Retinopathy of prematurity and associated factors. Int. Ophthalmol. Clin. *39*, 29–48.

Smith, L.E. (2004). Pathogenesis of retinopathy of prematurity. Growth Horm. IGF Res. *14*(*Suppl A*), S140–S144.

Smith, L.E. (2008). Through the eyes of a child: understanding retinopathy through ROP the Friedenwald lecture. Invest. Ophthalmol. Vis. Sci. *49*, 5177–5182.

Smith, L.E., Wesolowski, E., McLellan, A., Kostyk, S.K., D'Amato, R., Sullivan, R., and D'Amore, P.A. (1994). Oxygen-induced retinopathy in the mouse. Invest. Ophthalmol. Vis. Sci. *35*, 101–111.

Soker, S., Takashima, S., Miao, H.Q., Neufeld, G., and Klagsbrun, M. (1998). Neuropilin-1 is expressed by endothelial and tumor cells as an isoform-specific receptor for vascular endothelial growth factor. Cell *92*, 735–745.

Stahl, A., Connor, K.M., Sapieha, P., Willett, K.L., Krah, N.M., Dennison, R.J., Chen, J., Guerin, K.I., and Smith, L.E. (2009). Computer-aided quantification of retinal neovascularization. Angiogenesis *12*, 297–301.

Stahl, A., Connor, K.M., Sapieha, P., Chen, J., Dennison, R.J., Krah, N.M., Seaward, M.R., Willett, K.L., Aderman, C.M., Guerin, K.I., et al. (2010). The mouse retina as an angiogenesis model. Invest. Ophthalmol. Vis. Sci. *51*, 2813–2826.

Stefater, J.A., 3rd, Lewkowich, I., Rao, S., Mariggi, G., Carpenter, A.C., Burr, A.R., Fan, J., Ajima, R., Molkentin, J.D., Williams, B.O., et al. (2011). Regulation of angiogenesis by a non-canonical Wnt-Flt1 pathway in myeloid cells. Nature *474*, 511–515.

Stefater, J.A., 3rd, Lewkowich, I., Rao, S., Mariggi, G., Carpenter, A.C., Burr, A.R., Fan, J., Ajima, R., Molkentin, J.D., Williams, B.O., et al. (2011a). Regulation of angiogenesis by a non-canonical Wnt-Flt1 pathway in myeloid cells. Nature *474*, 511–515.

Stefater, J.A., 3rd, Ren, S., Lang, R.A., and Duffield, J.S. (2011b). Metchnikoff's policemen: macrophages in development, homeostasis and regeneration. Trends Mol. Med. *17*, 743–752.

Stein, E., Zou, Y., Poo, M., and Tessier-Lavigne, M. (2001). Binding of DCC by netrin-1 to mediate axon guidance independent of adenosine A2B receptor activation. Science *291*, 1976–1982.

Stewart, M.W. (2012). The expanding role of vascular endothelial growth factor inhibitors in ophthalmology. Mayo Clin. Proc. *87*, 77–88.

Tabas, I. (2010). The role of endoplasmic reticulum stress in the progression of atherosclerosis. Circ. Res. *107*, 839–850.

Tabas, I., and Ron, D. (2011). Integrating the mechanisms of apoptosis induced by endoplasmic reticulum stress. Nat. Cell Biol. *13*, 184–190.

Tadagavadi, R.K., Wang, W., and Ramesh, G. (2010). Netrin-1 regulates Th1/Th2/Th17 cytokine production and inflammation through UNC5B receptor and protects kidney against ischemia-reperfusion injury. J. Immunol. *185*, 3750–3758.

Tajiri, S., Oyadomari, S., Yano, S., Morioka, M., Gotoh, T., Hamada, J.I., Ushio, Y., and Mori, M. (2004). Ischemia-induced neuronal cell death is mediated by the endoplasmic reticulum stress pathway involving CHOP. Cell Death Differ. *11*, 403–415.

Tesfamariam, B. (1994). Free radicals in diabetic endothelial cell dysfunction. Free Radic. Biol. Med. *16*, 383–391.

van Rooijen, N., and van Kesteren-Hendrikx, E. (2002). Clodronate liposomes: perspectives in research and therapeutics. J. Liposome Res. *12*, 81–94.

van Rooijen, N., and van Kesteren-Hendrikx, E. (2003). "In vivo" depletion of macrophages by liposome-mediated "suicide". Methods Enzymol. *373*, 3–16.

Wang, W., Reeves, W.B., and Ramesh, G. (2009). Netrin-1 increases proliferation and migration of renal proximal tubular epithelial cells via the UNC5B receptor. Am. J. Physiol. Renal Physiol. *296*, F723–F729.

Wilson, B.D., Ii, M., Park, K.W., Suli, A., Sorensen, L.K., Larrieu-Lahargue, F., Urness, L.D., Suh, W., Asai, J., Kock, G.A., et al. (2006). Netrins promote developmental and therapeutic angiogenesis. Science *313*, 640–644.

Wong, C.H., Jenne, C.N., Lee, W.Y., Léger, C., and Kubes, P. (2011). Functional innervation of hepatic iNKT cells is immunosuppressive following stroke. Science *334*, 101–105.

Xu, C., Bailly-Maitre, B., and Reed, J.C. (2005). Endoplasmic reticulum stress: cell life and death decisions. J. Clin. Invest. *115*, 2656–2664.

Yang, X., Xin, W., Yang, X.M., Kuno, A., Rich, T.C., Cohen, M.V., and Downey, J.M. (2011). A2B adenosine receptors inhibit superoxide production from mitochondrial complex I in rabbit cardiomyocytes via a mechanism sensitive to Pertussis toxin. Br. J. Pharmacol. *163*, 995–1006.